Nonlinear effects in macroscopic kinetics

A. G. Merzhanov and É. N. Rumanov

Chernogolovka Branch of the Institute of Chemical Physics, Academy of Sciences of the USSR

Usp. Fiz. Nauk **151**, 553–593 (April 1987)

Macroscopic kinetics describes relaxation in terms of macroscopic states, i.e., the distributions of density, temperature, and so on. Two types of system are examined in this review, namely, (1) closed systems (or systems interacting exclusively with a thermostat) and (2) flow systems in which the nonequilibrium state is maintained by an external agency (source of supply or pump). In both cases, states are established that do not depend (in a particular range) on the initial conditions. These are the attractor states. Spatially homogeneous states (kinetic phases) are discussed for flow systems, together with transitions between them that are the analogs of the motion of interphase boundaries. In closed systems, the establishment of equilibrium can be preceded by the appearance of other attractors in the form of intermediate asymptotic behavior. A comparison is made between similar states in different processes (chemical reactions, viscous flows, absorption of light, and so on). Stability conditions are discussed.

CONTENTS

Introduction 293
1. Explosive instability 295
   1.1. Thermal and chain ignition. 1.2. Breakdown in dielectrics. 1.3. Induction. 1.4. Focal explosion. 1.5. Extinction. 1.6. Stabilization and stratification. 1.7. "Tricritical" point.
2. Progressive solitary waves 300
   2.1. Relaxation and switching waves. 2.2. Separation phenomena. 2.3. Flow reactor. 2.4. Light-induced combustion. 2.5. Interphase boundary. 2.6. Ignition.
3. Diffusional instability of relaxation waves 305
   3.1. Hydrodynamic and diffusional instabilities. 3.2. Cellular structures. 3.3. In-phase oscillations. 3.4. Spin states. 3.5. Complication and stochastization.
4. Multizone structure of progressive waves 309
   4.1. Two-zone combustion wave. 4.2. Multizone waves. 4.3. Wide zones. 4.4. Gasification. 4.5. Filtration waves. 4.6. Melting of porous material. 4.7. Thermal wave in a flow of helium.
Conclusion 314
References 314

> "*...in a pun two truths lie hid under one expression, so in an analogy one truth is discovered under two expressions.*"
> J. C. Maxwell

INTRODUCTION

In 1928, N. N. Semenov published a paper[1] on chain and thermal ignition. This was the beginning of the concept of explosive instability in chemistry. The course of a reaction was found to change abruptly as the parameters of the system (for example, the temperature) were varied continuously. Subsequent studies of the relationship between reactions and transport processes revealed the phenomena of bistability and hysteresis in chemical systems.[2,3] The theory of combustion waves[4] showed how a moving structure evolved in a distributed system, where the velocity and other parameters of the wave were determined by the state of matter and did not depend, within wide limits, on the manner of excitation (in modern terminology, this is an attractor). D. A. Frank-Kamenetskiĭ[5] then combined these and a number of other results, and proposed a new subject, namely, macroscopic chemical reaction kinetics.

Macrokinetics investigates reactions under real conditions in which they must be considered together with transport processes. A reaction produces a change in the concentration of reagents and in the temperature (because of the release of heat), whereas the rate of the reaction itself depends on temperature and the concentrations. Mathematically, the problem is to find the distributions of temperature and concentration (which, in general, are functions of time). In the corresponding equations of thermal conduction and diffusion, chemical reactions are represented by sources that are nonlinear functions of the required quantities. In many natural and artificial systems, reactions are accompanied by the flow of the medium. Convective trans-

0038-5670/87/040293-24$01.80

port, usually much more effective than diffusion, is then brought into play. On the other hand, reactions influence the flow because of the relationship between viscosity, on the one hand, and chemical composition and temperature, on the other.

Theoretical and experimental studies of interactions between all these factors have led to considerable advances in macrokinetics (see, for example, the second edition of Frank-Kamenetskiĭ's book[5] and Ref. 6). Some of the results will be discussed below. For the moment, we must draw attention to another aspect of the problem. Even in his original paper,[1] N. N. Semenov, in his treatment of thermal explosions, cites the study of breakdown in dielectrics at high temperatures, reported in Ref. 7. For a given voltage, there is a reciprocal relationship between current and Joule heating (because of the increase in conductivity with temperature), and a similar relationship between the exothermic reaction rate and heating. In both cases, this leads to a disruption of the thermal balance of the system. An analogous explosive instability was subsequently investigated theoretically[8] and experimentally[9] for the flows of a very viscous liquid (the reciprocal relation is then assured by the strong temperature dependence of viscosity). For a pulsed discharge in a gas, the expansion of the current channel was interpreted in Ref. 10 as an analog of flame propagation. This analogy was extensively exploited in Ref. 11 in relation to discharges in different frequency ranges. In one of his last papers,[12] D. A. Frank-Kamenetskiĭ called for a comparative study of processes occurring in plasmas and chemical systems. A collection of the analogs of combustion in different processes is given in Refs. 13 and 14.

From the theoretical point of view, there is no justification for singling out processes involving chemical reactions. The standard definition of a macroscopic state (in terms of the distribution of thermodynamic variables such as density, concentration, pressure, temperature, velocity, and so on, in a continuous medium) implies that there is a science that investigates relaxation in the language of macrostates. This is, in fact, macroscopic kinetics, and it is precisely in this wide sense that we shall use the terminology first introduced by D. A. Frank-Kamenetskiĭ. Unfortunately, the ground covered by this definition is immense. In the present paper, we shall pursue a more realistic goal, i.e., we shall compare chemical and nonchemical processes, and discuss some typical nonlinear effects exhibited by these processes.

We shall consider two types of nonequilibrium systems. In a closed system (or a system that interacts only with a thermostat), nonlinearity gives rise to a number of phenomena that accompany the transition to equilibrium (self-acceleration, evolution of inhomogeneities, relaxation waves, and so on). The second type includes systems in which the nonequilibrium state is maintained by external factors (source of supply or pump). We shall refer to them as flow systems. While equilibrium is established in a closed system in the course of time, the evolution of a flow system ends when it reaches an "attractor" state whose parameters do not depend (in a certain sense) on the initial conditions. In the case of relaxation of a closed system, an attractor regime that is different from equilibrium can only be observed in the form of the so-called intermediate asymptotic behavior[30] with a limited lifetime.

The space of the parameters of a flow system splits into regions belonging to different attractor regimes (these regions may, in fact, partially overlap). As the parameters vary, a rearrangement occurs when the boundary of a particular region is reached, i.e., there is a transition to another attractor regime. This rearrangement occurs because, within its own region, the old regime is unstable against appropriate small perturbations. While equilibria are the subject of thermodynamics, the basic task of macrokinetics is to investigate attractor regimes and their rearrangement.

Like plasmas, nonequilibrium chemical systems exhibit a variety of instabilities. Studies of thermal instability[1-3] were further advanced in Refs. 15 and 16 where, in particular, thermokinetic oscillations were investigated. Postulation of the hydrodynamic instability of laminar flames[17,18] led to extensive searches for stabilization mechanisms (see Ref. 19). The problem of diffusional instability of combustion waves is closely approached in Ref. 20 (see also Ref. 21). The result of the nonlinear stabilization of these instabilities is the experimentally observed cellular flame[22] or, in condensed systems, self-oscillatory[23,24] and spin[24] combustion.

An important contribution to macrokinetics was the discovery of self-oscillatory and spatially inhomogeneous states in the Belousov-Zhabotinskiĭ reaction.[25] An important class of nonlinear electrochemical phenomena, that includes the propagation of nerve pulses (see, for example, Ref. 26), has been investigated, but only to a very limited extent. "Unifying concepts," such as autowaves (see Refs. 27, 28, and so on), dissipative structures and self-organization,[29,30] synergetics,[31] and catastrophe theory[32] have been widely discussed in recent years in relation to a variety of nonlinear effects in nonequilibrium (active) systems.

It has become clear that the subject is getting closer to the modern (nonlinear) theory of oscillations.[33] A detailed investigation of the simple diffusional instability model has led to a large number of solutions describing "kinetic heterostructures," their pulsations, and randomization[34-36,6] (Vol. 1, Part 1, p. 3). This range of problems has been adequately treated in the review literature, and we will not go into it in any detail. To keep our review to manageable proportions, we have also had to leave out the consideration of interesting effects such as "chemical" free convection,[37] the interrelation between reactions and viscosity in flow systems,[38] gas-dynamic interruption of reactions leading to the formation of a quasiperiodic structure on the detonation front,[39] and so on.

We begin by considering explosive instability in homogeneous and metastable states and in stationary regimes. We shall examine the conditions necessary for the appearance of inhomogeneities and the coexistence of kinetic "phases" in flow systems. A particular type of inhomogeneity is the progressive solitary wave, first investigated in Refs. 4, 40, and 41. A solitary wave maintains an exact balance between supply and dissipation (similarly to the way in which a soliton maintains precise compensation between nonlinearity and dispersion[42]). Sections 3 and 4 are devoted to the structural complication of solitary waves. One of the reasons for this complication is the above-mentioned diffusional instability and its nonlinear stabilization.[43-47] The banded structure of waves can be due to a sequence of reactions,[48,49] phase transitions,[50,51] filtration in porous media,[52,53] and other factors.

The present state of our knowledge in the field of nonlinear kinetic effects is such that a more or less arbitrary selection has to be made from the vast available information (in other words, the authors' interests constitute a significant factor). Nevertheless, we hope that our review will serve as an introduction to this frontier of physics, which closely approaches chemical physics and biophysics. We are grateful to A. P. Aldushin and Ya. B. Zel'dovich for useful discussions.

1. EXPLOSIVE INSTABILITY

In the simple case of a single reaction in a stationary medium, we have the following two equations:

$$\frac{\partial T}{\partial t}=\chi\Delta T+Q\Phi(\eta,\ T), \tag{1.1}$$

$$\frac{\partial\eta}{\partial t}=D\Delta\eta+\Phi(\eta,\ T); \tag{1.2}$$

where T is the temperature, η is the so-called transformation depth, which is zero for initially pure material and 1 for the reaction products, χ is the thermal diffusivity, D is the diffusion coefficient, Φ is the reaction rate ("frequency" of elementary events), and Q is the heat of the reaction per unit specific heat c. We shall consider exothermic reactions, i.e., $Q>0$.

1.1. Thermal and chain ignition

For many reactions, the dependence of Φ on η can be represented by the factor $(1-\eta)^n$, where n is a positive number of the order of unity. At the initial stage of the reaction, when $\eta\ll 1$, this factor is of little significance and we can confine our attention to the single equation (1.1) with $\Phi(0,T)$. As far as the stability of stationary regimes is concerned (the heat released in the reaction is completely removed from the system), the long-wave modes are the most "hazardous." It is therefore sufficient to confine our attention to the equation averaged over the volume:

$$\frac{dT}{dt}=Q\Phi(T)-\alpha S(\rho cV)^{-1}(T-T_0), \tag{1.3}$$

where V, S are the volume and the surface area of the vessel containing the medium, respectively, T_0 is the temperature of the thermostat, α is the effective heat transfer coefficient, and ρ is the density.

The Semenov diagram shown in Fig. 1 illustrates the temperature dependence of the two terms on the right-hand side of (1.3). The dependence of Φ on T is basically of the activation type, i.e., $\Phi\sim\exp(-\varepsilon/T)$, which is the Arrhenius law. It is clear that, of the two[1)] stationary points, only the low-temperature point (1) is stable. As the temperature T_0 increases, the two points approach one another and merge (broken line a). When $T_0>T_a$ (broken line b), we have accelerated heating (thermal explosion), independently of the dependence on the initial temperature of the medium.[2)] Suppose, however, that the condition for an explosion

$$\varkappa=Q\varepsilon V\rho c\,(T_0^2\alpha S)^{-1}\,ke^{-\varepsilon/T_0}>\frac{1}{e} \tag{1.4}$$

is not satisfied, and the temperature is constant ($T=T_1$). The best known reason for the self-acceleration of a reaction in this case is chain branching.[1]

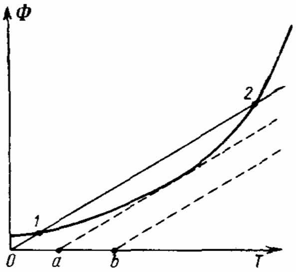

FIG. 1. Semenov diagram: ignition occurs when the initial temperature of the reagents is higher than T_2 or the temperature of the thermostat is higher than T_a.

A reaction (especially in the gas phase) practically never reduces to the direct transformation of the initial materials into reaction products (the cross section for this process is too low). The initial stage is the formation of intermediate active particles (free radicals, ions). These particles then enter new reactions in which final products and new active particles are produced. These active particles "multiply" in the branched chain reaction. For example, the oxidation of hydrogen involves the following sequence of reactions:[54]

$$\left.\begin{array}{r}\mathrm{OH}+\mathrm{H_2}\rightarrow\mathrm{H_2O}+\mathrm{H},\\ \mathrm{H}+\mathrm{O_2}\rightarrow\mathrm{OH}+\mathrm{O},\\ \mathrm{O}+\mathrm{H_2}\rightarrow\mathrm{OH}+\mathrm{H},\\ \cdots\cdots\cdots\cdots\end{array}\right\} \tag{1.5}$$

Some of the radicals are lost to the walls and in chain-breaking reactions within the volume. If we regard η as the concentration of active particles (for example, H), and if we use the boundary condition

$$(D\nabla_\perp\eta+k_w\eta)_s=0, \tag{1.6}$$

where $\nabla_\perp\eta$ is the normal component of the gradient on the surface and k_w is the reaction rate on the (heterogeneous) surface, spatial averaging of (1.2) finally yields

$$\frac{d\eta}{dt}=K_0+K_1\eta,\quad K_1=2K_+-K_--K_wSV^{-1}; \tag{1.7}$$

where K_0 is the rate of spontaneous production of the radicals H under the influence of light, collisions of the second kind, and so on, K_+ and K_- are the rate of the second[3)] reaction in (1.5) (branching) and the rate of loss in reactions within the volume, respectively,

$$K_w=k_w\,(1+k_w\rho\beta^{-1})^{-1} \tag{1.8}$$

is the renormalized rate of the heterogeneous reaction, $\beta\sim\rho DSV^{-1}$ is the mass transfer coefficient, and K_1 is a function of the concentrations of the other components in the mixture. The linearity of (1.7) is entirely due to the quasistationary approximation.

The avalanche increase in η (chain ignition) occurs for $K_1>0$ when the rate at which new radicals are produced is greater than the rate at which they are lost. Since $K_+\sim P$ and $K_-\sim P^2$ (P is the pressure), the chain explosion corresponds to a relatively narrow pressure interval[56] (Fig. 2).

It was suggested in Ref. 57 that explosive instability is always a chain or thermal process. In an active medium consisting of excited molecules, a thermal "explosion" will develop if the rate of deactivation increases with temperature[58] (the "chain channel" of instability then corresponds to the laser pulse). In a flow of a very viscous liquid, the heat generated by friction tends to reduce viscosity (which falls with

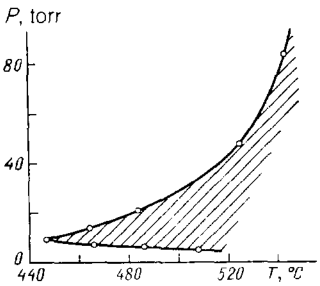

FIG. 2. Region of chain ignition of an explosive mixture (shaded) on the P, T plane (data taken from Ref. 56).

temperature), a considerable amount of heat is released as a result of the increase in velocity, and so on, so that the explosive instability sharply alters the energy transfer from the external source that maintains the given flow.[8,9] An analogous feedback situation leads to the self-acceleration effect during the baking of fine metallic powders, in which the excess surface energy is the source of energy.[59]

1.2. Breakdown in dielectrics

A clear example of a process demonstrating explosive instability is that of a current flowing in a dielectric. As in all other cases, where a very complex phenomenon takes place, we shall treat breakdown from the "macrokinetic" standpoint.

Figure 3 shows a typical temperature dependence of the breakdown voltage U of a solid dielectric. There are two well-defined regions, namely, the high-temperature region in which $U^2 \sim \exp(-\varepsilon/T)$ and the activation energy ε is the same as for the conductivity of the given medium,[7] and the low-temperature region in which $U(T)$ is a slowly-varying function. It was shown in Refs. 7 and 61 that pure "thermal breakdown" occurs at high temperatures. To describe the thermal instability, it is convenient to use Fig. 1 and (1.3) in which $Q\Phi$ is replaced with $\sigma E^2(\rho c)^{-1}$, where σ is the conductivity and E the field strength. A condition analogous to (1.4) shows that U falls exponentially with T. For specimens in the form of sufficiently thin plates, for which α is independent of the thickness d (external heat transfer), we find that $U \sim d^{1/2}$, which is also in agreement with experiment.

At low temperatures, the field necessary for the development of thermal instability turns out to be too high, and breakdown is due to collisional ionization. Electrons accelerated out of the conduction band by the applied field acquire sufficient energy to eject further electrons from the valence band, and so on. At the same time, collisions with phonons lead to energy losses and, in the final analysis, to recombination. The modern theory of collisional ionization is developed in Refs. 62 and 63. In the stationary state, the electron and hole densities n_e and n_h are determined from the equations

$$n_{0e}(E, T) + [w_{ie}(E) - w_{re}(E)]\, n_e + w_{ih} n_h = 0, \quad (1.9)$$

$$n_{0h}(E, T) + [w_{ih}(E) - w_{rh}(E)]\, n_h + w_{ie} n_e = 0, \quad (1.10)$$

where n_{0e} and n_{0h} are the rates at which electrons and holes are produced by thermal ionization and are directly removed by the field (tunnel effect), and w_i, w_r are the average ionization and recombination probabilities (evaluated using the nonequilibrium distribution function found in Ref. 62).

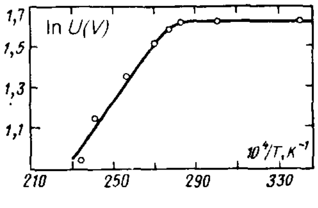

FIG. 3. Temperature dependence of the breakdown voltage of porcelain.[60]

Comparison of (1.9) and (1.10) with the right-hand side of (1.7) shows that low-temperature breakdown constitutes a "chain explosion" in the number of carriers. The probability w_r decreases with increasing field (in accordance with a power-type law), while the relative number of slow electrons decreases and so does the recombination rate. The probability w_i increases exponentially with increasing field [in weak and moderate fields, this is basically $\exp(-\mathrm{const}/E)$, whereas in strong fields the variation is $\exp(-\mathrm{const}/E^2)$, which corresponds to the "diffusion" of electrons in energy space[63]]. Once $w_i(E)$ and $w_r(E)$ are known, they can be used in (1.9) and (1.10) to find the breakdown field E_c.

Because of the drift of carriers in the field E, the instability that leads to "chain" breakdown is, in general, convective. In a solid dielectric, the convective nature of the instability is not very significant because both types of carrier produce ionization. The breakdown condition is[62]

$$(f_e - f_h)\, d = \ln \frac{f_e}{f_h}, \quad (1.11)$$

where f is the ionization coefficient (ratio of w_i to the drift velocity), so that d is only a logarithmic function of f_e/f_h. In low-pressure gases, secondary avalanches result (according to Townsend) in the bombardment of the cathode by positive ions, whereas at high pressures they result in photochemical ionization (see Ref. 64).

1.3. Induction

If, instead of (1.4), the strong inequality $\varkappa \gg 1$ is satisfied, the time taken for the temperature to rise from T_0, i.e., the induction period, is shown by (1.3) to be

$$\tau_1 \approx T_0^2 (Q\varepsilon k)^{-1} e^{\varepsilon/T_0}. \quad (1.12)$$

The significant point is that, when $T_0 \ll \varepsilon$, the main contribution to τ_1 is provided by the low-temperature stage of the reaction (so long as its acceleration is small). This means that we can ignore the complicated subsequent stages of the process when we use the estimate given by (1.12).[4] Condition (1.4) can be conveniently written as $\tau_1 < \tau$, where $\tau \sim V\rho c(S)^{-1}$ is the characteristic time for heat transfer to the thermostat.

Figure 4 shows the time dependence of the temperature difference $T - T_0$ for the liquid in the gap between a fixed outer cylinder and a rotating inner cylinder.[9] The experiments were performed at fixed torque, so that the rotational frequency increased during the dissipative heating, the viscosity fell in accordance with the expression $\nu \sim \exp(\varepsilon/T)$, and there was a corresponding increase in the power supplied by the source. Substituting this power $\sim \sigma^2 \nu^{-1}$ (σ is the tangential stress) for $Q\Phi$ in (1.3), we obtain a thermal

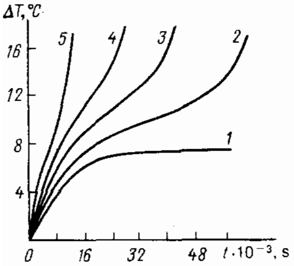

FIG. 4. Heating of castor oil in the gap between two concentric cylinders. Thermostat temperature: 1—8.8; 2—11.1; 3—12.2; 4—14; 5—20 °C.

instability condition that is similar to (1.4). For the parameters of the system used in Ref. 9, this condition becomes $T_0 > 9.8$ °C, in agreement with Fig. 4. The curves shown in Fig. 4 are similar to the thermograms of a typical exothermic reaction with one exception: in the region of thermal stability (curve 1), the heating-up of the chemical systems tends to zero for $t \to \infty$ because the system burns out.

For chain ignition, (1.7) shows that the concentration growth rate is K_1. For explosion to take place, the nonlinear terms must not suppress instability. For example, if we add the term $K_2\eta^2$ to the right-hand side of (1.7), we must have $K_2 \geqslant 0$. For chain reactions, nonlinear amplification is assured by the so-called positive chain interaction (see Ref. 65). When $K_2 \ll (K_1^2 K_0^{-1})$, the induction period is

$$\tau_i \approx K_1^{-1} \ln \frac{K_1^2}{K_0 K_2}\,. \tag{1.13}$$

When the spontaneous chain nucleation rate K_0 is low enough, the delay of the explosion fluctuates, depending on the random value of the initial concentration.[159]

Autocatalysis of an exothermic reaction can lead to an explosion even when (1.4) is not satisfied,[66] and the thermal state is stable. However, the accumulation of active material increases the reaction rate Φ. The $\Phi(T)$ curve of Fig. 1 tends to rise, and, at a certain instant of time, the condition for thermal instability is satisfied for the temperature of the system. The explosion therefore occurs in two stages, namely, the autocatalytic and the thermal. The low-temperature breakdown of solid dielectrics is also found to conclude with the thermal stage.

1.4. Focal explosion

Suppose that a certain portion of a combustible mixture is suddenly heated to a temperature T. If the linear size of the region is $l > l_0$, where

$$l_0 \sim [\chi\tau_1(T)]^{1/2}, \tag{1.14}$$

the reaction will accelerate more rapidly than the rate at which heat is lost. The result will be the focal explosion investigated in Ref. 68. During the time $t \sim \tau_1$, the ambient medium remains cold but, at the center of the heated region, the temperature rises without limit ("intensified state" in the terminology used in Ref. 69). Figure 5 reproduces the temperature distributions calculated in Ref. 70 for a reactive sample (diameter d) heated on the surface. It is clear that, as dl_0^{-1} increases, the "intensified" temperature peak shifts from the center to the periphery. Comparison of (1.4), (1.12), and (1.14) shows that, when $\alpha \sim \rho c \chi d^{-1}$, we have $\varkappa \sim [d/l_0(T_0)]^2$. The quantity l_0 is well-known in combustion theory (see, for example, Section 119 of Ref. 71). It is referred to as the "correlation length" in Ref. 69.

Inhomogeneities in the initial temperature distribution become intensified in the course of the explosive heating if their size is[72] $l \gtrsim l_0$. This appears to have a significant influence on the structure of the detonation front. The exothermic reaction zone follows the density discontinuity in the detonation wave, and sets up the initial conditions for the explosion. Deviations from the homogeneous temperature distribution immediately after the discontinuity become intensified and form "hot spots" on the front (these are the foci of intensive reactions), which serve as the sources of secondary detonation waves. The result of this is that a complicated quasiperiodic structure replaces the plane front.[39]

1.5. Extinction

In a closed chemical system,[5)] explosive instability accelerates the transition to equilibrium. We now turn to flow systems. Suppose that an exothermic reaction occurs only on a surface in contact with a flowing mixture with fixed concentration $1 - \eta$ of initial material. We then have[2]

$$\Phi = K_w (1 - \eta) S V^{-1}, \tag{1.15}$$

where K_w is given by (1.8). Since $k_w \sim \exp(-\varepsilon/T)$, the $\Phi(T)$ curve is S-shaped and is such that $\Phi \sim \exp(-\varepsilon/T)$ (kinetic region); at high temperatures, it approaches asymptotically the constant value $S\beta(\rho V)^{-1}$ (diffusional region). Substituting (1.15) in (1.3), we obtain the following expression for the stationary state:

$$[Q(1 - \eta) - \alpha(\beta c)^{-1}(T - T_0)]k_w = \alpha(\rho c)^{-1}(T - T_0). \tag{1.16}$$

The graphical solution of (1.16) is shown in Fig. 6, where the stationary points 1 and 2 are similar to the corresponding points in Fig. 1. The new, high-temperature point 3 (diffusional state) is stable, so that bistability occurs for a particular range of the parameters. When the parameters are varied (for example, α is varied), the ignition process that we have already described (point 1 coalesces with the unstable point

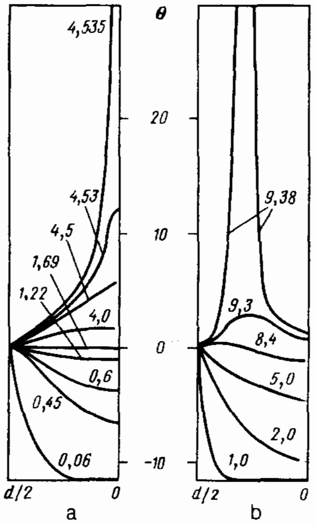

FIG. 5. Temperature distribution during surface heating, shown for successive instants of time: the numbers against the curves are the values of $t/\tau_j(T_0)$. $(d/l_0)^2 = 8$ (a) and 20 (b).

2) can occur side by side with the reverse transition (from the diffusional to the kinetic state), i.e., we have extinction[2] in which points 2 and 3 coalesce.

A picture analogous to Fig. 6 (bistability and hysteresis) is also found to occur in the case of a volume reaction.[3] The conditions at entry and exit provide the contribution $(T-T_0)\tau_0^{-1}$ to the right-hand side of (1.3), where τ_0 is the time spent by the medium in the flow reactor in which the temperature at entry is the thermostat temperature. Correspondingly, it follows from (1.2) that

$$\frac{d\eta}{dt}=(1-\eta)\,ke^{-\varepsilon/T}-\eta\tau_0^{-1}, \tag{1.17}$$

where it is assumed that the order of the volume reaction is $n=1$ and, at entry, $\eta=0$. In the stationary state [cf. (1.16)]

$$[Q\rho cV\,(\rho cV+\alpha S\tau_0)^{-1}-(T-T_0)]\tau_0 ke^{-\varepsilon/T}=T-T_0. \tag{1.18}$$

The dependence of the left-hand side of (1.18) on T is the same as in (1.16). Moreover, if we consider thermal states for different values of τ_0, we find that, in addition to the S-shaped portion of the $T(\tau_0)$ curve, a closed $T(\tau_0)$ curve splits off from the low-temperature branch in a certain range of parameter values.[160] The closed curve lies above the low-temperature branch, but only its upper arc is stable. Spontaneous transitions from the low-temperature branch to the state corresponding to the isolated curve are not, of course, possible. On the other hand, outside the bistable region, when only the low-temperature stationary state is possible, the reactor temperature can rise to values typical for the high-temperature state for suitably chosen initial conditions. Extensive transformation of the reagents then takes place, the reactor cools down, and is filled with new material, eventually reaching the stationary state.[161]

The stationary flow of a viscous liquid in a tube of length L is described by

$$\nu\left(\frac{v}{d}\right)^2=(\alpha d^{-1}+\rho cvL^{-1})\,(T-T_0), \tag{1.19}$$

$$PL^{-1}=\nu vd^{-2}, \tag{1.20}$$

where P is the pressure drop and d^2 is the cross-sectional area of the tube (numerical coefficients depend on the shape of the cross section, and are omitted). Eliminating the velocity v, we obtain[73]

$$[P-\rho c\,(T-T_0)]\,P\nu^{-1}\left(\frac{d}{L}\right)^2=\alpha d^{-1}(T-T_0), \tag{1.21}$$

which is also similar to (1.16) and (1.18) when $\nu\sim\exp(\varepsilon/T)$. When the temperature T_{in} of the liquid at entry is greater than T_0, bistability may occur in cooling states[74] even when the heat due to friction is not taken into account. Actually, if we replace (1.19) with

$$\alpha d^{-1}\,(T-T_0)+\rho cvL^{-1}\,(T-T_{in})=0 \tag{1.22}$$

we find that

$$\rho c\,(T_{in}-T)\,P\nu^{-1}\left(\frac{d}{L}\right)^2=\alpha d^{-1}(T-T_0). \tag{1.23}$$

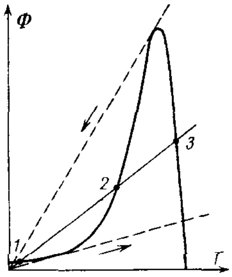

FIG. 6. Thermal steady-states in a flow system. The bistability region lies between the broken lines.

The presence of the reverse transition (extinction) in the flow system is due to the fact that both stable states (points 1 and 3 in Fig. 6) are nonequilibrium states, whereas, in a closed system, the explosive decay of the metastable state concludes with transition to equilibrium. We now mention a few examples of bistability in flow systems. The thermal state of a cloud of interstellar gas cooled by radiation is considered in Ref. 75. The energy input is provided by cosmic radiation. Two stable states with different degrees of gas ionization are then possible for given intensity of this radiation. The thermal balance of material heated by a current is determined by the equations

$$\sigma E^2=\sigma^{-1}j^2=\alpha SV^{-1}\,(T-T_0), \tag{1.24}$$

so that, if $\sigma(T)$ is S-shaped, we have thermal bistability in a given field E, whereas, if the curve $\rho(T)=\sigma^{-1}$ is S-shaped, the bistability occurs at constant current j. The former case corresponds to melting or a polymorphic transformation in solid dielectrics and semiconductors,[76] and the second to a transition of a superconductor to the normal phase. The bistability of a dielectric during melting in a high-frequency field was first noted in Ref. 77 (it was reported in Ref. 78 for the dc case). It was noted for the polymorphic and superconducting transitions in Refs. 79 and 80, respectively.

Concentrational bistability is possible under isothermal conditions. Analysis of the creation of electron-hole pairs in a semiconducting film (under the influence of laser radiation) and of their recombination has shown that there are two concentrations that are stable against small perturbations in a given light flux: for the lower concentration, the medium is a semiconductor, whereas for the higher—a semimetal. Bistability with respect to the presence of Cooper pairs (see Ref. 82) is possible when a superconducting film is illuminated: one stationary state corresponds to a superconductor and the other to a normal metal.

1.6. Stabilization and stratification

The role of illumination (or some other way of affecting concentration) is reduced in Refs. 81 and 82 to a shift of the phase equilibrium point. The phases themselves remain (at least qualitatively) as the phases of the medium in equilibrium. By analogy, stationary states in other flow systems with bistability, that were discussed above, can be referred to as "kinetic phases." One of the first papers in which this analogy was noted appears to be the review in Ref. 83. Hysteresis in such "phase transitions" is similar to hysteresis due to heating and supercooling. Let us now consider spatially inhomogeneous states in flow systems that are the analogs of "phase equilibrium."

We begin with the thermal states of a nonlinear resistor,[83] described by (1.24). If the function $\sigma(T)$ is S-shaped, then, as shown in Section 1.5, bistability occurs under the conditions for a constant voltage. The current-voltage characteristic $j(E)$ of the specimen is also S-shaped (there is a region $E_d < E < E_u$ in which for each value of E there are three values of T and, consequently, three values of j). If we stabilize the current flowing through the specimen (for example, by connecting a large constant resistor in series with the nonlinear resistor), the current distribution over the cross section of the specimen is nonuniform for $\partial j/\partial E < 0$. Two regions are formed (hot and cold "phases"), separated by a relatively narrow transition layer, in which the temperature drop is concentrated. The voltage across this "two-phase" specimen is determined by the condition for a stationary temperature field, from which it follows that (see below, Section 2.1).

$$\int_{T_1}^{T_3} [\sigma(T) E^2 - \alpha S V^{-1} (T - T_0)] \, dT = 0, \qquad (1.25)$$

where T_1, T_3 are the temperatures of the "phases" (cf., Fig. 6). Equation (1.25) resembles the condition for the coexistence of liquid and vapor (Maxwell's rule), which determines the position of the horizontal segment of the van der Waals isotherms. The distribution of the cross-sectional area of the sample among the phases depends on the given total current in accordance with the "lever rule"

$$\langle j \rangle = [\sigma(T_1) x + \sigma(T_3)(1 - x)] E, \qquad (1.26)$$

where $\langle j \rangle$ is the ratio of the current and the cross-sectional area, x is the fraction of the cross section that corresponds to the cold phase, and E is determined from (1.25).

In the case of the S-shaped function $\sigma^{-1}(T)$, the current-voltage characteristic of the specimen is N-shaped and the coexistence of phases occurs when the voltage is stabilized in the range $\partial j/\partial E < 0$. The specimen becomes stratified into regions of strong and weak field at right angles to the current.[84] The current in the two-phase state is constant, and the ratio of the layer widths is determined by the given voltage.

It follows from (1.19)–(1.23) that, in liquids with the standard dependence $\nu \sim \exp(\varepsilon/T)$, thermal instability leads to an S-shaped relationship between the pressure head and the rate of flow,[73,74] where the high-temperature state is due to convective transport of heat.[73,85] If, instead of considering the distributed system, we take the simpler point system in the form of a bifurcating tube[85] (or two parallel resistors[86]), then stabilization of the flow rate is not accompanied by division into "phases" and, instead, there is a change in flow symmetry: one tube is hotter than the other, and the greater proportion of the fluid flows through it. As the flow rate increases, symmetry is broken when $\tau_1 \sim \tau$, but is then restored when $\tau \sim \tau_0 = Lv^{-1}$. The symmetry breaking occurs in the soft state, and symmetry restoration in the hard state.[85]

In a chemical flow system, the stabilization of thermal instability can be achieved experimentally in the so-called compensated electrothermograph.[87] The working part of this device is a platinum wire stretched across the flowing reagents at temperature T_0. According to (1.16) and Fig. 6, for exothermic catalysis, there are two possible stable homogeneous states on the surface of the wire, namely, diffusional and kinetic states. The temperature of the surface, on which the rate of catalysis depends, is stabilized by the current flowing through the wire. This current is varied by a tracking system so as to maintain a given value of the wire resistance (which is a function of temperature). It is found[88] that, for certain particular values of the resistance, the reaction rates exhibit discontinuities, and this is interpreted in Ref. 88 as isothermic ignition and extinction. It is shown in Ref. 89 that these results correspond to the appearance of an inhomogeneous thermal state (Fig. 7).

The inhomogeneous state is characterized by the temperature distribution along the wire shown schematically in Fig. 7. The kinetic "phase" occupies the region near the electrodes, where there are better conditions for cooling. The diffusional "phase" lies between them. Since the resistance of platinum is a slowly-varying function of temperature, and in this particular temperature range this relationship is in any event nearly linear, the more convenient quantity, namely, the mean temperature of the wire $\langle T \rangle$, is shown along the ordinate axis in Fig. 7. In the inhomogeneous state,

$$\langle T \rangle L = T_3 L_3 + T_1 (L - L_3), \qquad (1.27)$$

where L is the length of the wire, L_3 is the width of the diffusional "phase," and T_1, T_3 are the temperatures of the "phases." These temperatures remain practically constant as the average temperature $\langle T \rangle$ is varied, and (1.27) is satisfied by shifting the "phase boundaries" by varying L_3. The current I in the inhomogeneous state is almost independent of L_3 and is given by

$$\int_{T_1}^{T_3} \left[\rho c Q \Phi + \sigma^{-1} \left(\frac{IL}{V} \right)^2 - \alpha S V^{-1} (T - T_0) \right] dT = 0, \qquad (1.28)$$

which resembles (1.25).

The transitions shown by the vertical arrows in Fig. 7 correspond to ignition and extinction, discussed in Section 1.5. The "isothermal ignition" is a transition from the kinetic to the inhomogeneous state with the formation of a hot segment (arrow from A_2 to the line CD in Fig. 7). In the reverse transition, i.e., isothermal extinction, the hot segment disappears (arrow from D to the line A_1A_2).

The segment B_1C corresponds to the "supercooling" of the diffusional phase. Since the ends of the wire are in con-

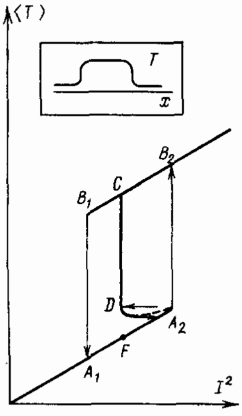

FIG. 7. Average temperature evaluated over the length of the wire in the compensated electrothermograph as a function of the square of the current. A_1A_2 and B_1B_2 are the kinetic and diffusion branches, CD is the coexistence line for the kinetic and diffusion "phases." Broken line shows the result for the unstable "nucleus" of the diffusion state.

tact with the cold electrodes, this supercooling is impossible: if we take the system to the region CB_2 and then reduce the current (without stabilizing $\langle T\rangle$), then, as we approach C, the "nuclei of kinetic phase" that are present at the ends will ensure a transition to the kinetic state (to the point F). The segment FA_2 corresponds to the "heating" of the kinetic phase. This means that the "nucleus of the diffusional phase" (heated region) will grow under these conditions.[6)]

1.7. "Tricritical" point

Let us now follow Ref. 86 and consider the case illustrated in the box of Fig. 8. The resistors R_1, R_2 (they have identical electric and thermophysical parameters) depend on temperature in accordance with the expression $\exp(\varepsilon/T)$, but the ballast resistor R_0 is temperature-independent. Let us determine the currents I_1, I_2 for given voltage U. Since we have two variable resistors, we can investigate particularly simply the nonsymmetric states that are analogous to the coexistence of kinetic phases (mentioned in Section 1.6). By varying R_0, we can smoothly go over from fixed voltage across the working resistance (when $R_0 \to 0$) to fixed current ($R_0 \gg R_1, R_2$).

The behavior of this system can be described by the two thermal-balance equations

$$\frac{d\theta_i}{d\tau} = \varkappa e^{\theta_i}[1+\rho(e^{\theta_1}+e^{\theta_2})^2]^{-2} - \theta_i \quad (i=1,\ 2), \tag{1.29}$$

where $\theta_i = \varepsilon(T_i - T_0)T_0^{-2}$, $\tau = t\alpha S(Mc)^{-1}$, M is the mass of the working resistor,

$$\rho = \frac{R_0}{R_i(T_0)}, \quad \varkappa = \varepsilon(\alpha S T_0^2)^{-1}\frac{U^2}{R_i(T_0)}, \tag{1.30}$$

and the parameter $\varkappa$ is similar to the Semenov number (1.4). Figure 8 shows the subdivision of the $\varkappa$, ρ plane into the different "phases." The case $\rho = 0$, when the equations in (1.29) are independent, was considered in the theory of thermal breakdown,[7] in which breakdown ($\theta_i \to \infty$) occurs for $\varkappa = 1/e$. When ρ is arbitrarily small, but not zero, the discontinuity in the current (finite for $\rho \neq 0$) is accompanied by the appearance of asymmetry ($\theta_1 \gg \theta_2$ or $\theta_2 \gg \theta_1$). In other words, only one of the two resistors breaks down, which is in qualitative agreement with the experiment reported in Ref. 7, in which a sharp spatial inhomogeneity was observed in the breakdown phenomenon.

Transitions between symmetric and asymmetric states exhibit hysteresis, as shown in Fig. 8. As ρ increases, the region of bistability becomes narrower, and vanishes altogether at $\rho_* \simeq 0.0786$. When $\rho > \rho_*$, the transition to the asymmetric state is not accompanied by a current discontinuity. Instead, there is a singularity of the form

$$I - I_c = \text{const}\cdot(U - U_c)^{1/2}. \tag{1.31}$$

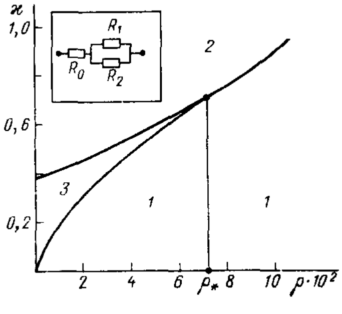

FIG. 8. Kinetic "phase diagram" for a circuit consisting of three resistors: 1—symmetric state; 2—asymmetric states; 3—bistability.

The above effects resemble first-order phase transitions (jumps and hysteresis) for $\rho < \rho_*$ and second-order transitions for $\rho > \rho_*$. Accordingly, the point $\varkappa_c(\rho_*)$ in Fig. 8 plays the part of a "tricrital" point. In other cases, for example, for "phase transitions" corresponding to (1.16), (1.18), (1.21), and (1.23), the difference between "phases" of the same symmetry (homogeneous phases) vanishes at the "critical" point. The above equations can also be written in the form

$$(T_m - T)Ke^{-\varepsilon/T} = T - T_0, \tag{1.32}$$

where T_m and K are constants. The critical point is then determined by the condition

$$T_m = T_0\left[1 - \left(\frac{4T_0}{\varepsilon}\right)\right]^{-1}. \tag{1.33}$$

The existence of the critical point (1.33) enables us to execute a continuous transition between the high-temperature and low-temperature states, i.e., a transition without jumps (ignition and extinction) via the post-critical region of the parameter values. A transition between states of different symmetry is not possible. This is the reason for the line of soft rearrangement and the tricritical point of Fig. 8.

The connection between the symmetry of attracting states and the subdivision of the space of the parameters into regions belonging to these states was demonstrated here by considering the simple example of stationary points. On the other hand, it is quite obvious that this relationship is general in character. The structure of the space of the parameters of the flow system depends on the symmetry of the attracting states to the same extent that the shape of the thermodynamic phase diagram depends on the symmetry of existing phases.

2. PROGRESSIVE SOLITARY WAVES

We saw in Sections 1.6 and 1.7 that, under certain conditions, the development of explosive instability will result in spatially inhomogeneous states. Progressive solitary waves, which constitute traveling inhomogeneities, are among the striking phenomena studied in macrokinetics. They were first described theoretically in Refs. 4, 40, and 41 in relation to the propagation of a dominant gene and combustion waves. It is shown in Ref. 4 that the velocity of uniform motion of a flame relative to the burning material has a particular "intrinsic" value. When the undamped motion of a hydrodynamic soliton is due to the precise compensation of nonlinearity and dispersion effects,[42] the energy spent in heating the initial material in the combustion wave is compensated by the release of heat in the chemical reaction zone. Moreover, in contrast to solitons in a medium without dissipation, the interaction between the solitary waves considered here is not at all similar to "elastic collisions." Interactions will be examined in Section 4; for the moment, we confine our attention to a single propagating wave.

2.1. Relaxation and switching waves

Let us consider (1.1) and (1.2) in a infinite medium and seek their self-similar solutions that depend only on the argument $x + ut$, i.e., we confine our attention to the case of a plane wave propagating from right to left along the x-axis. The initial reagents lie ahead of the wave front and the hot reaction products are left behind. Accordingly, in the coordinate frame in which the wave is at rest, we have the following equations:

$$\chi T'' - uT' + Q\Phi(\eta, T) = 0, \tag{2.1}$$

$$D\eta'' - u\eta' + \Phi(\eta, T) = 0 \tag{2.2}$$

and boundary conditions

$$x \to -\infty, \quad T = T_0, \ \eta = 0, \tag{2.3}$$

$$x \to +\infty, \quad T' = 0, \ \eta' = 0. \tag{2.4}$$

As in Section 1.1, the function $k(1-\eta)^n \exp(-\varepsilon/T)$ can serve as a model for $\Phi(\eta, T)$. From the mathematical point of view, the problem defined by (2.1)–(2.4) is not completely correct. Because of the small but finite reaction rate at $T = T_0$, the transformation will occur in a sufficiently distant region before the reaction "wave" reaches that region. The phrase "intermediate asymptotic behavior" is therefore used in this connection.[90] To avoid introducing the finite dimensions of the specimen, it is convenient to neglect the source in (2.1) and (2.2) in the low-temperature region, as in done in Ref. 4. The combustion wave is then found to consist of two zones, namely, the heated zone and the reaction zone (Fig. 9). In the heated zone

$$T = \text{const}\cdot e^{ux/\chi}, \quad \eta = \text{const}\cdot e^{ux/D}, \tag{2.5}$$

so that the influx of heat and reaction products into the fresh mixture is independent of the coefficients χ, D, and is a function of only the velocity u and the values $T(x=0)$ and $\eta(x=0)$ on the boundary between these zones. Because the source is an exponential function of temperature, the reaction zone is narrow in comparison with the heated zone, and the zone-width ratio is $l_R/l_C \sim \Gamma = T_0 T_f(\varepsilon Q)^{-1}$, where $T_f = T_0 + Q$ is the temperature of the products. The mean temperature in the reaction zone is close to T_f, and the product concentration is close to $\eta_R = \exp(-\Gamma\chi D^{-1})$, which corresponds to the extrapolation of (2.5) to this narrow zone.[91] The rate of flow of heat out of the reaction zone is of the order of $\rho c Q\Phi(\eta_R, T_f)l_R$. Using (2.5), we find that the wave velocity is approximately given by

$$u^2 \sim \Gamma\chi\Phi(\eta_R, T_f). \tag{2.6}$$

A definite "intrinsic" value of u is obtained because the problem defined by (2.1)–(2.4) is invariant under translation along the x axis. Since the solution then contains an arbitrary constant (which depends on the choice of the origin of coordinates), one of the conditions, (2.3) or (2.4), is redundant. It can be used to determine the wave velocity.

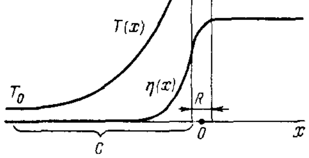

FIG. 9. Structure of combustion wave: C—heated zone; R—reaction zone. The profile $\eta(x)$ corresponds to $D < \chi$.

The wave propagation mechanism is as follows. The reaction is accelerated when the initial material receives the heat that is rapidly released in the reaction occurring in the heated medium. The propagation of a chain-reaction wave in a highly diluted, slightly heated (cold flame) mixture was discovered in Ref. 92. Isothermal propagation is due to the diffusion of active particles from the reaction zone into the initial medium. In both cases (chain and thermal propagation), the initial mixture of reagents is metastable, but equilibrium is established behind the wave. Such waves can be referred to as relaxation waves.

As mentioned above, to obtain a unique solution of the problem defined by (2.1)–(2.4), we must neglect reactions at low temperatures.[4,5,91] The excitation of the waves in this way must be hard (see Section 2.6). A continuous spectrum of wave velocities with a lower bound is obtained in Refs. 40, 41, where an analysis is made of the initial state that was unstable against small perturbations. High velocities are obtained for a "smeared out" initial distribution of active-particle concentration, and the propagation of this kind of wave is a phase effect due to the delay of instability development in distant portions of the system.[91] Nonstationary (nonuniform) motion of the waves, due to the reaction at the initial temperature is investigated in Refs. 163 and 164. A model source is used in Ref. 164 to analyze the behavior of the lower bound of the velocity spectrum between the limiting cases considered in Refs. 4 and 40.

A relaxation wave can propagate in the "active medium" produced by exciting the molecules of the material from the equilibrium state (to vibrational or electronic levels). Such processes are considered in Ref. 58 (wave of thermal deactivation in a vibrationally excited gas) and in Ref. 93 (wave of thermal quenching of luminescence). The wave of thermal recombination of free radicals (nitrogen atoms deposited on a liquid helium film) is investigated experimentally in Ref. 94. Frontal crystallization of a highly supercooled liquid (in which the velocity of the interphase boundary was an increasing function of its temperature) is studied in Ref. 95.

In detonation waves, the heating of the original medium is produced not as a result of thermal conduction but by a shock wave. However, for all types of progressive solitary waves in closed nonequilibrium systems (or systems interacting with a thermostat), these are relaxation waves that take metastable material to equilibrium. We now turn to flow systems. To begin with, we shall suppose that the corresponding states include a spatially homogeneous (and stationary) state. When the conditions are such that there is bistability, the inhomogeneous state described in Section 1.6 (coexistence of kinetic "phases") is possible. The position of the inhomogeneity, i.e., of the interphase boundary, can be stabilized (in the same way that, for the temperature and pressure corresponding to the phase equilibrium, the mass ratio of these phases is set by fixing the volume). In general, the inhomogeneity is not at rest. Let us consider the uniform motion of the boundary in a bistable system. We shall follow Ref. 96, in which the following equation is given for a heterogeneous reaction on a wire stretched across a current of freshly prepared mixture:

$$\chi T'' - uT' + Q\Phi(T) - \mathrm{Nu}\,\chi d^{-2}(T - T_0) = 0, \qquad (2.7)$$

where the source Φ is given by (1.15), the boundary conditions are

$$x \to -\infty, \quad T = T_1; \quad x \to +\infty, \quad T = T_3, \qquad (2.8)$$

T_1, T_3 are the temperatures of the kinetic and diffusional states, respectively (see Fig. 6), d is the wire diameter, and Nu is the Nusselt number.

One value of the velocity u in the problem defined by (2.7) and (2.8) corresponds to each set of parameters in the bistability region. When

$$\int_{T_1}^{T_3} F(T)\,\mathrm{d}T = 0, \quad F(T) = Q\Phi(T) - \mathrm{Nu}\chi d^{-2}(T - T_0) \qquad (2.9)$$

we have $u = 0$. A "phase transformation" occurs when the integral in (2.9) is not zero, and the direction of this transformation (the sign of u) is the same as the sign of (2.9). So long as the integral in (2.9) is small, we have

$$u \sim \frac{d}{\mathrm{Nu}^{1/2}}(T_3 - T_1)^{-2} \int_{T_1}^{T_3} F(T)\,\mathrm{d}T. \qquad (2.10)$$

Both directions of propagation of the thermal wave are possible because both homogeneous states (before and ahead of the wave) are nonequilibrium states. Such waves are called switching waves. A large number of switching waves in different bistable systems is described in the literature. They include ionization and recombination waves in the interstellar gas,[75] waves of transition between a semiconductor and a semimetal,[79,81] or between a superconductor and a normal metal,[80,82] waves of transition between bubble and film boiling states,[97] and so on. Figure 10 shows examples of the measured switching-wave velocity as a function of the supplying thermal source (current). The graph in Fig. 10a is in qualitative agreement with (2.10), whereas in Fig. 10b there is a plateau for $u = 0$. A plateau is also observed in other systems in which it is probably due to slight stabilization by inhomogeneities[98] (in contrast to the stabilization described in Sections 1.6 and 1.7).

2.2. Separation phenomena

In contrast to switching waves whose velocity can be either positive or negative, depending on the parameter values, the velocity of relaxation waves is always positive. Moreover, we always have $u \geqslant u_t$, where u_t is a threshold velocity. The presence of thresholds was found in Ref. 99, where an analysis was given of a flame propagating along a tube (diameter d). The narrow reaction zone can be regarded as a surface on which

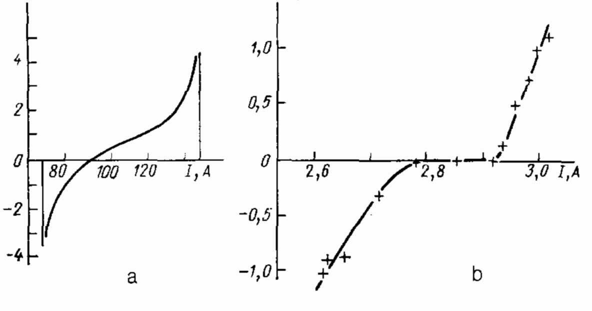

FIG. 10. Velocity of switching waves supplied with Joule heat: a—motion of the boundary between a superconductor and normal metal[80]; b—transition between film and bubble boiling states[97] with the wire heater immersed in water.

$$\chi(T'_{-0} - T'_{+0}) = Qu. \qquad (2.11)$$

The temperature gradients T'_{-0}, T'_{+0} are determined by

$$\chi T'' - uT' - \mathrm{Nu}\chi\, d^{-2}(T - T_0) = 0, \qquad (2.12)$$

which is valid everywhere except for $x = 0$, and by the condition

$$T(x = \pm\infty) = T_0, \quad T(+0) = T(-0). \qquad (2.13)$$

To close the problem defined by (2.11)–(2.13), we must also provide the relationship between the velocity u and the temperature $T(x = 0) = T_\mathrm{m}$, which is given by the internal solution. Let us suppose that

$$u^2 = \mathrm{const}\cdot\exp(-\varepsilon/T_\mathrm{m}) \qquad (2.14)$$

[cf. (2.6)]. The equation for u, obtained by eliminating T_m from these equations, will, in general, have three roots, say u_1, u_2, and u_3 in order of increasing value. The solution corresponding to u_2 is unstable. The root u_1 is redundant: for velocities as low as this $[(u_1/u_3) \sim \exp(-\varepsilon/2T_0)]$, we must take into account the reaction at $T = T_0$, and there is no wave solution. It is significant that, when

$$d^2 \approx 2e\mathrm{Nu}\,\chi^2 Q\varepsilon\,(u_0 T_t)^{-2}, \qquad (2.15)$$

in which $u_0 = u(d \to \infty)$, the stable root u_3 merges with u_2 and vanishes. At the point of merging $u = u_t \simeq u_0/e^{1/2}$. Heat losses reduce the velocity of the combustion wave, but not to zero, and separation (extinction) occurs for $u = u_t$. The separation mechanism can be reduced to positive feedback[99] between the temperature T_m and velocity u. The velocity falls when T_m is reduced, and the loss of heat increases, which leads to a further reduction in T_m, and so on (see also Ref. 91).

The velocity of an isothermal flame, propagating as a result of the diffusion of active particles into the fresh mixture, was calculated in Ref. 100. It was shown that also in this case separation occurred for a finite (nonzero) velocity as a result of the merging of stable and unstable solutions (see also Ref. 101). The reason for separation is the loss of active particles to the tube walls (see Section 1.1). When the wave velocity is reduced, the diffusion current to the walls, which is responsible for the losses, is found to increase, while the maximum concentration of radicals (in the flame) falls. Consequently, the reaction slows down, there is a further reduction in the wave velocity, and so on.

The motion of a plane crystallization front toward a supercooled amorphous phase is discussed in Ref. 95. Instead of (2.14), we then have

$$u = \mathrm{const}\cdot e^{-\varepsilon/2T_\mathrm{m}}\left(e^{-Q/T_\mathrm{m}} - e^{-Q/T_\mathrm{e}}\right), \qquad (2.16)$$

which represents, approximately, the velocity of the interphase boundary as a function of its temperature T_m, the temperature of phase equilibrium T_e, and the latent heat Q. At low enough temperatures, (2.16) and (2.14) are practically indistinguishable. As before, eliminating T_m with the aid of (2.11)–(2.13), we obtain u as a function of the initial temperature T_0, which is schematically illustrated in Fig. 11. Of course, $u = 0$ when $T_0 = T_e$. The velocity increases in the course of supercooling, but separation occurs at $T_0 = T_A$, and u falls discontinuously to an exponentially small value. This separation is similar to the combustion limit discussed in Ref. 99. During heating to $T_0 = T_B$, the motion of the boundary accelerates abruptly.

2.3. Flow reactor

When the excitation rate is low, a flow system may be regarded as approximately closed over limited intervals of time. As we have seen, switching waves occur in flow systems, and relaxation waves in closed systems. The velocity of the latter has a threshold. To elucidate the relationship between these two types of solitary wave, we consider again the exothermic flow reactor as an example. As noted in Section 1.5, there is a definite range of parameter values in which there are two stable homogeneous states, namely, the high-temperature and the low-temperature ones. Switching waves propagating in the lateral direction (relative to the supplying flow) accomplish the transition between these states. On the other hand, when the parameters are such that only the low-temperature (homogeneous) state is possible, the medium filling the reactor at a given time can be "ignited." The resulting wave is a relaxation wave that leaves behind the reaction products. The weak supplying flow then ensures that the initial state (cold fresh mixture) is restored well behind the wave front. Thus, in addition to the homogeneous state, there is also the inhomogeneous state, i.e., a propagating pulse,[102] whose leading edge is the relaxation wave.

Let us now take the x axis at right-angles to the supplying flow, to achieve maximum simplification, let us take the length of the reactor along the x axis to be infinite, and assume instantaneous mixing in the axial direction. Instead of (2.1) and (2.2), we then obtain

$$\theta''_{\xi\xi} - v\theta'_{\xi} + \mu\gamma^{-1}(1-\eta)\,e^{\theta} - \theta\,(\gamma\varkappa)^{-1} = 0, \tag{2.17}$$

$$v\eta'_{\xi} = \mu\,(1-\eta)\,e^{\theta} - \eta; \tag{2.18}$$

where $\xi = x/(\tau\chi)^{1/2}$, τ is the time spent by the medium in the reactor, $\theta = \varepsilon(T - T_0)T_0^{-2}$, $v = u(\tau/\chi)^{1/2}$, $\mu = \tau K(T_0)$, K is the reaction rate constant, $\gamma = T_0^2/\varepsilon Q$, $\varkappa^{-1} = \gamma(1 + \tau\tau_d^{-1})$, and $\tau_d = d^2/N\chi$ is the characteristic time for heat transfer across the reactor walls. The transport of material along the x axis will be neglected, the relevant condition for this being $D \ll \chi$. As before, we assume that $\gamma \ll 1$.

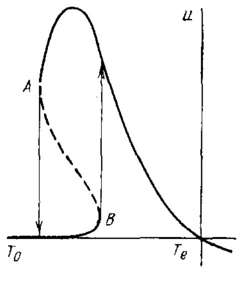

FIG. 11. Velocity u of the crystallization front[95] as a function of the initial temperature of the amorphous phase T_0. Broken curve—unstable solution.

The subdivision of the plane of the parameters μ, $\varkappa$ for homogeneous states[5] is shown in Fig. 12a. The line AD corresponds to the coexistence of the kinetic "phases" (2.9), which takes the form

$$\mu = e^{-\varkappa/2}. \tag{2.19}$$

In the region BAD, the high-temperature state is the "more stable," whereas in the region CAD the low-temperature state is the "more stable." The ignition line AB and extinction line AC play the role of kinetic spinodals. When $\varkappa \gg 1$, the equations for these lines assume the simple form:

$$\mu \approx (e\varkappa)^{-1}, \quad \mu \approx \varkappa e^{-\varkappa}, \tag{2.20}$$

respectively. The critical point A has the coordinates $\varkappa = 4$, $\mu = e^{-2}$. The velocity of the switching waves is $v = 0$ along the line (2.19). When $v \ll (\gamma\varkappa)^{1/2}$, we can neglect the left-hand side of (2.18), as is done in Ref. 96. Eliminating η, we obtain a source of the form (1.15) in (2.17). The solutions for this case are described at the end of Section 2.1.

Below the line AC, the boundary conditions for (2.17) and (2.18) with $\mu \ll 1$ are

$$\xi = \pm\infty, \quad \eta \approx \mu, \quad \theta \approx \varkappa\eta. \tag{2.21}$$

The structure of the traveling pulse includes a heated zone, a reaction zone, and a cooling zone, in which θ and η return to the values given by (2.21). When $\gamma\varkappa \ll 1$, cooling is faster than the influx of the fresh mixture, i.e., when $\eta \simeq 1$, the traveling pulse "reduces" to a relaxation wave.[7)] A calculation analogous to that given in Section 2.2 yields the following estimate for the separation boundary:

$$\mu \approx 2e\gamma^{-3}\varkappa^{-1}e^{-1/\gamma} \tag{2.22}$$

(the line E_1E_2 in Fig. 12a). When γ is small enough, the line E_1E_2 lies below the bistability region ABC. Consequently, both switching waves and traveling pulses correspond to the parameters belonging to this region. Figure 12b shows schematically the function $v(\mu)$ for given $\varkappa$, where OH is the traveling-pulse branch and $O'O''$ is the branch corresponding to the switching wave. The separation for $\mu = \mu_1$ is analogous.[99] At O', the switching wave is abruptly transformed into a traveling pulse because of competition between the terms $v\eta'_{\xi}$ and $-\eta$ in (2.18).

When the switching wave propagates toward the low-temperature state (ignition wave), the reaction transforms

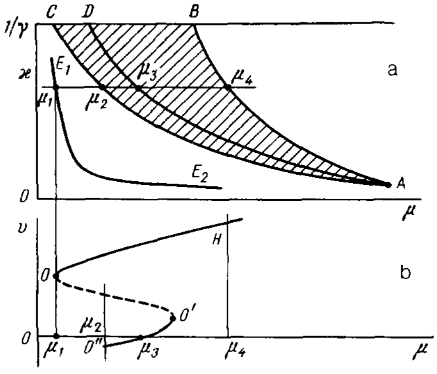

FIG. 12. The states of the flow reactor: a—plane of the parameters (bistable region shown shaded); b—v as a function of μ for given $\varkappa$. Unstable solution shown by the broken line.

not only the materials entering the reactor, but also the fresh mixture lying along the path of the wave in the cold part of the reactor. The faster the wave propagation, the greater is the fraction of this "additional supply" that acts as positive feedback for the system. Hence, the self-acceleration of the wave ends discontinuously at the point O'.

The difference between a traveling wave front, for which the states of the medium ahead of the solitary wave and behind this wave are different, and a traveling pulse behind which the initial state is restored, has frequently been emphasized in the literature (see Refs. 27, 28, 157, 165). From the point of view of the properties of solitary waves, it seems to us that the most significant point is whether a given wave is a relaxation wave, for which the velocity can change sign, or a relaxation wave, which has a velocity threshold. In particular, points representing $v(\mu < \mu_2)$ on the branch OH in Fig. 12b correspond to a solution in the form of a wave for which the initial low-temperature state is restored behind the wavefront, whereas points representing $v(\mu > \mu_2)$ correspond to the situation where the high-temperature homogeneous state $\theta = \theta_3 \simeq \varkappa (< 1/\gamma)$ is established in the bistability region behind the front, in which the temperature θ is close to $1/\gamma$. This change in the wave structure at $\mu = \mu_2$ does not lead to a significant change in the wave velocity because the change is largely confined to the "rear" of the solitary wave.

When $\mu_2 < \mu < \mu_3$, the switching wave takes the reactor from the high-temperature to the low-temperature state, and this can be interpreted as a consequence of the "metastability" of the high-temperature state. However, for the same values of μ, it is possible to excite a relaxation wave whose propagation is accompanied by the replacement of the low-temperature state by the high-temperature state.

2.4. Light-induced combustion

We now turn to the case of "longitudinal" propagation in which the solitary wave travels toward the energy-supplying flow (or recedes from it).

Examples of counter propagation include the motion of a plasma region that absorbs energy from a laser beam[103] and microwaves in a waveguide.[104] A receding wave is produced when fog is illuminated by a laser beam.[105] The evaporation front associated with absorbing droplets in fog leaves behind a transparent channel through which energy is supplied to the front. Analogous effects are produced when the reacting medium is eliminated: a counter wave is produced when the initial mixture is transparent and the reaction products are absorbed,[106] while an accompanying wave appears in the case of absorbing initial materials and transparent products.[107]

The velocity of these waves depends on the power supplied to the system, but they are structurally very close to relaxation waves. In this respect, the light-induced combustion wave,[103] i.e., absorbing plasma, produced by thermal ionization and propagating in the direction opposite to the incident beam, is of considerable interest. For simplicity, the absorption coefficient can be assumed to be zero[11] for $T < T_*$ and equal to the constant $\varkappa$ for $T > T_*$ ($T_* \sim 10^4$ K is the *somewhat arbitrary temperature at which absorption saturates*). When $\varkappa d \ll 1$ (d is the diameter of the light channel), and the motion is uniform, the plasma takes the form of a column lying along the beam. Well away from the end of the column, the heat release and the energy loss through the side surface are in balance:

$$\varkappa I\ (x) \approx \mathrm{Nu}\rho c \chi T d^{-2}, \qquad (2.23)$$

where $I(x)$ is the intensity at a distance x from the leading edge. The column is effectively bounded by two switching waves, namely, an ignition wave ahead of the column and an extinction wave at the rear. The length l of the column is determined by the condition that the two wave velocities be equal, i.e., $u[I(0)] = -u[I(l)]$. The velocities are given by formulas such as (2.10). However, this picture is useful only when the length l is large enough.

Calculations of the interaction between the wavefronts have shown[108] that the dependence of the light-induced combustion velocity on the parameter $s = I(0)\varkappa d^2 (N\rho c\chi T_*)^{-1}$ have two branches that merge when

$$s_t \approx 17 \left(1 + \frac{\varkappa d}{\mathrm{Nu}^{1/2}}\right), \quad u_t \approx 0{,}2\chi \left(d + \frac{\mathrm{Nu}^{1/2}}{\varkappa}\right)^{-1}. \qquad (2.24)$$

The lower of these branches is unstable,[109] which is fully analogous to the results obtained for relaxation waves (see Section 2.2). Since $\varkappa$ increases with increasing pressure P, (2.24) shows that the threshold intensity I_t initially falls as a function of P and then reaches a constant value, which is in qualitative agreement with the data reported in Ref. 110.

Studies of an optical discharge in a flowing gas[111] have revealed a nonmonotonic (including a minimum) dependence of the threshold power on the gas velocity u. This result is interpreted[108] as a consequence of the two-valuedness of the function $u(s)$. Since the lower branch of $u(s)$ is unstable, a different explanation must be found. It may be considered (in agreement with Ref. 111) that, when $u < u_t$, the plasma is displaced from the lens focus in the forward direction. This produces an increase in d, so that $u = u_t(d)$, and the threshold power $\sim I_t(d) d^2$ increases.

2.5. Interphase boundary

As in Section 2.2, the fact that the reaction-zone width is small enables us to subdivide the combustion wave problem into an external and an internal problem. The internal solution gives a nonlinear boundary condition that closes the external problem. The same procedure is used to solve the problem of the motion of the interphase boundary. The boundary has an atomic width, so that the solution of the internal problem that is necessary to obtain (2.16) lies outside the framework of macrokinetics. This solution is obtained in Ref. 112 for a medium near the critical point, in which the width of the boundary is a "macroscopic" quantity (of the order of the correlation radius of fluctuations) and the van der Waals equation is valid. We shall write this equation in the form

$$p = 4t + 6tr + \frac{3}{2} r^3 - G r''; \qquad (2.25)$$

where $p = (P - P_c)P_c^{-1}$, $r = (\rho - \rho_c)\rho_c^{-1}$, $t = (T - T_c)T_c^{-1}$, the subscript c refers to variables evaluated at *the critical point, a phase difference can occur only for $t < 0$,* and the numerical coefficients are chosen in accordance with the law of corresponding states. The last term on the right-hand side is necessary if we are to describe the inhomogeneity, i.e., the interphase boundary. The definition of the internal problem implies that $t = \text{const}$ ($T = T_m$; see Section 2.2). Combining (2.25) with the condition for one-dimensional stationary continuity and the Navier-Stokes equations

$$\rho v = \rho_0 u, \quad P - P_0 + \rho_0 u\,(v - u) = \nu v', \tag{2.26}$$

where v is the flow velocity, the subscript 0 refers to the state ahead of the boundary, i.e., within the internal scale $x = -\infty$, $\nu = (4/3)\eta + \zeta$, η, ζ are the first and second viscosities, and transforming to the dimensionless coordinate $\xi = x(-tG^{-1})^{1/2}$, we obtain

$$\theta_{\xi\xi} - gU\theta_\xi = -(U^2 + 6)(\theta - \theta_0) + \frac{3}{2}(\theta^3 - \theta_0^3); \tag{2.27}$$

where $\theta = r/(-t)^{1/2}$, $g = \nu(\rho_c P_c G)^{-1/2}$, and $U = u[\rho_c/(-tP_c)]^{1/2}$. The boundary conditions

$$\theta\,(\xi = -\infty) = \theta_0, \quad \theta_\xi\,(\xi = +\infty) = 0 \tag{2.28}$$

are satisfied only for certain definite ("eigen") values of U, which depend on θ_0.

In contrast to the formulation of the problem given in Refs. 81, 82, which is close to (2.27) and (2.28), the right-hand side of (2.27) depends on the velocity U because we have taken into account the momentum balance (2.26). The phase boundaries examined in Ref. 81 (semiconductor-semimetal) and in Ref. 82 (superconductor-normal metal) propagate under the influence of light that produces a nonequilibrium quasiparticle concentration. The absorbed energy is dissipated in the form of noncoherent recombination radiation (into excitons and Cooper pairs, respectively). The boundary propagates as a switching wave, and the given light intensity determines the densities of both phases (bistability) in accordance with the conditions for equilibrium between pair creation and recombination. As far as the propagation of the boundary between metastable and equilibrium phases [defined by (2.27) and (2.28)] is concerned, the density in the final state (equilibrium phase), $\theta(\xi = \infty) = \theta_2$, is not given and must be found together with the velocity. It is only for $U \to 0$, i.e., in the case of small supersaturation for which the change in pressure in the wave can be neglected, that θ_2 is determined by the equation of state. Similarly, in the case of slow combustion (when the wave velocity is small in comparison with the velocity of sound and the pressure is $P \simeq \text{const}$), the temperature T_f of the products is determined thermodynamically (see Section 2.1), whereas the state behind the fast combustion front depends on its velocity (see Ref. 71, Section 122). A gas-dynamic calculation of the final state is given in Ref. 166 for the decay of the metastable phase.

To be specific, we shall suppose that the metastable phase has the lower density. The range of variation of θ_0 between the binodal and spinodal is $(-2, -2/\sqrt{3})$, and $\theta_2 \geqslant 2$ (equilibrium phase). As was first shown in Ref. 113,

$$U = -3\sqrt{3}\,(2g)^{-1}\theta_1, \tag{2.29}$$

where θ_1 is a root (as are θ_0 and θ_2) of the polynomial on the right-hand side of (2.27). It is readily seen that, when $g^2 < 9/2$, the function $U(\theta_0)$ is two-valued in this region ($U > 0$). A rising branch passes through the phase equilibrium point $\theta_0 = -2$, $U = 0$; the solution corresponding to the other (descending) branch is unstable. For sufficiently fluid materials ($g < 2$), these branches merge at $\theta_0 = \theta_* < -2/\sqrt{3}$, and we again have the phenomenon of separation. We may suppose that inclusion of terms of higher order in r in (2.25) will lead to the appearance of a new branch with greater values of U, and the solution (2.29) undergoes an abrupt transition to this new branch at θ_{**}.

The onset of separation at θ_* can be explained as follows. The boundary is stationary when the chemical potentials of the two phases are equal, so that the phases are in equilibrium with each other. The velocity of the boundary increases with the difference $\Delta\mu$ between the chemical potentials of the equilibrium and metastable phases. Acceleration of the boundary is accompanied by an increase in the pressure of the equilibrium phase and in $\Delta\mu$, which leads to further acceleration, and so on.

The "initial" supersaturation θ_0 is found by solving the external (thermal) problem. The solution of the internal problem (see Section 2.2) together with (2.29) shows that, for a three-dimensional specimen, the temperature T_m of the boundary is almost equal to the phase equilibrium temperature T_e for all T_0. The velocity of the boundary is therefore small in comparison with (2.29), and depends neither on viscosity nor on thermal conductivity (Stefan state). It is only in one- and two-dimensional cases (films and filaments), for which $T_m \simeq T_0$, that the velocity is close to (2.29) (hydrodynamic state). For the crystallization front,[95] the transition from the Stefan to the hydrodynamic states in the two-dimensional system corresponds to supercooling $T_0 \lesssim T_e - Q$.

2.6. Ignition

The study of solitary waves is a relatively complicated task because the process is nonstationary and there is an obvious variety of initial conditions that lead to a given steady state. For relaxation waves, the unstable solution serves as the boundary of the attractor region, but only for one class of initial conditions. A reaction in a layer in contact with a hot surface was considered in an early paper.[114] It was assumed that ignition corresponded to the separation of the stationary thermal state. At the point of separation, the temperature gradient on the surface becomes equal to zero, i.e., the release of the heat of reaction in the boundary layer is completely compensated by its loss to the cold medium. It was assumed in Ref. 115 that ignition occurred when the heat yield of the reaction was equal to the heat input into the system. A numerical experiment was used in Ref. 116 to investigate the entire process of approach to combustion, and not just its initial stage. It was found that this approach was often accompanied by oscillations in the distribution of T and η. Oscillations were also observed in the experiments reported in Ref. 117 on the propagation of a combustion wave across the separation boundary between two types of solid fuel. The oscillations were probably due to the same mechanisms that were responsible for the instability of stationary waves, to which we now turn.

3. DIFFUSIONAL INSTABILITY OF RELAXATION WAVES

3.1. Hydrodynamic and diffusional instabilities

Hard decays of metastable states were examined in Section 1. As noted in Section 2.6, relaxation waves evolve to such states under certain definite (localized) interactions. In addition to separation phenomena (Section 2.2), relaxation waves exhibit diffusional instability that develops in the soft state, and also hydrodynamic instability. These instabilities were originally discovered by studying combustion waves. The hydrodynamic instability[17,18] appears as a consequence of the thermal expansion of the burning medium. If we look upon the combustion wave as a surface across which there is an abrupt change in density, the spectrum of the corresponding linearized problem is described by the following dispersion relation[17]:

$$\Omega^2(u_0 + u) + 2\Omega k u_0 u + k^2 u_0 u\,(u_0 - u) = 0, \qquad (3.1)$$

where u_0, u are, respectively, the unperturbed velocity of the original material and the velocity of the products (in the coordinate frame in which the wave is at rest and the unperturbed flow is a steady state one). Because of thermal expansion $u > u_0$ ensures that there is a root $\Omega > 0$. In accordance with (3.1), short waves grow more rapidly than long waves but, when $k \gtrsim u_0/\chi$, the wave can no longer be looked upon as a surface of discontinuity, and we must take into account its structure, as described in Section 2.1.

A new (diffusional) instability is revealed when the structure is taken into account. Qualitative ideas explaining the origin of this instability were first put forward in Ref. 21. Let us suppose that the ratio of the diffusion coefficient and thermal diffusivity is $\mathrm{Le} = D/\chi \gg 1$. The protrusion that appears on the plane surface of the flame is then in an "advantageous" position: the fresh mixture arrives in the reaction zone more rapidly than heat leaves this zone. The temperature in the reaction zone becomes higher and, at the same time, there is an increase in the rate of combustion on this part of the front. The protrusion runs forward, and the curvature of the front increases. We shall see in Section 3.2 that both instabilities can be stabilized by the same factors.

When $\mathrm{Le} < 1$, the ratio of the diffusion and thermal fluxes from the reaction zone is such that it tends to suppress the curvature of the front. Calculations of the stability limit[118] confirm these qualitative considerations. Moreover, studies of the diffusional instability[119,120] have shown that, when $\mathrm{Le} = 0$ (see also Ref. 43), the instability also occurs in the region $s > 4$, where

$$s = Q\frac{\partial \ln u}{\partial T_f} \qquad (3.2)$$

is the so-called temperature coefficient of velocity. The position of the limit of stability on the Le, s plane is shown in Fig. 13 (taken from Ref. 121). According to this figure, there are two instability regions (I and II). The boundaries of these regions approach the $\mathrm{Le} = 1$ line asymptotically as $s \to \infty$. When $\mathrm{Le} = 1$, it is clear from (2.1)–(2.4) that the η and $T - T_0$ profiles are similar, and one of the equations (2.1) and (2.2) can be eliminated. In the case of a single equation, the monotonic solution describing the combustion wave is always stable.[122] The mechanism responsible for the instability in region I was discussed above. The instability in region II is probably generated by structural features on the combustion wave for $\mathrm{Le} < 1$: because there is little diffusion, the heated layer ahead of the reaction zone is virtually free of combustion products. The front can propagate rapidly through a heated fresh mixture of this kind, and then comes to rest before the cold medium (see Ref. 20). Instability to curvature is a secondary effect: when the separation between two portions of the front is much greater than the characteristic length $l_0 \sim \chi/u$, the two cannot influence one another and the "phases" of their motion are, in general, different.[19]

The growth-rate spectra calculated in Ref. 119 are in agreement with the above discussion.[19] All the spectra terminate ($\mathrm{Re}\,\Omega$ passes through zero) for a finite value $k = k_0$, where k_0 is of the order of l_0^{-1}. At the same time, in region I we have $\Omega \sim k^2$ for $k \to 0$, and in region II the growth rate remains finite for long-wave modes.8) When stability was investigated in Refs. 118–120 and elsewhere, the analysis was based on a simplified model of the combustion wave (see Section 2.2): the reaction zone was replaced by a surface on which the thermal and diffusion fluxes had a discontinuity. Instead of the "internal" solution, we can introduce a nonlinear boundary condition relating the temperature of the "surface" and the velocity of the wave. The dependence of velocity on temperature gradients is additionally taken into account in Ref. 121. The approximation involving an infinitesimally narrow reaction zone enables us to examine the spectra so long as $|\Omega| \ll \tau_R^{-1}$, where τ_R is the reaction time. The restrictions on the side of the short-wave modes are less significant because $k_0 < (\chi\tau_R)^{-1/2}$. We shall return to this question in Section 3.4.

Gas mixtures in which the concentration of the light reagent is lower than the stoichiometric value can serve as a model of a medium with $\mathrm{Le} > 1$. When a combustion wave propagates through a condensed medium, we have $\mathrm{Le} \ll 1$. We shall consider both these cases in the account that follows.

3.2. Cellular structures

The transformation of a laminar into a cellular flame was discovered in experiments[22] with gaseous mixtures (Fig. 14, taken from p. 265 of the book by Lewis and von Elbe[54]). The bright cells framed by darker boundaries have dimensions of the order of 1 cm. The mixture, whose flame was photographed, included nitrogen, oxygen, and butane. The concentration of the last of these was greater by a factor of 1.39 than the stoichiometric figure. Cellular structures have also been observed when butane was replaced with hydrocarbons in a comparatively wide range of pressures and other parameters. In all cases, the mixtures were depleted in the light reagent. It appears that the corresponding diffusion coefficient was higher than the thermal diffusivity of the mixture, so that the situation corresponded to region I in Fig. 13.

In this region,[118,121] the growth rate spectra exhibit a maximum at the wavelength $\sim 10\chi/u$. We may suppose that the behavior of the system is determined by the mode with the highest growth rate $\Omega(k_m)$ [other modes grow more

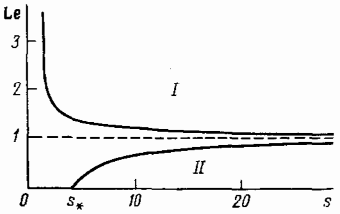

FIG. 13. Limits of stability of a plane combustion wave.

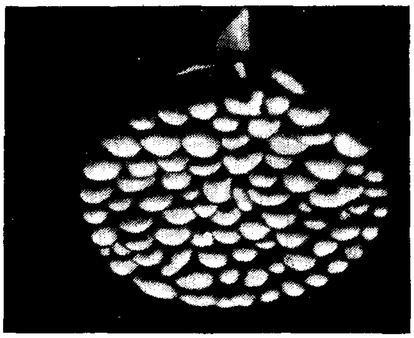

FIG. 14. Cellular structure of a flame. The photograph was taken at an angle from below. Pressure 414 torr.

slowly and their amplitudes eventually become negligible in comparison with $A(k_m)$]. On this assumption, the mechanism responsible for stabilization appears to be as follows.[123,124] Consider the curving of the front, for example, in accordance with the law sin $k_m y$, where the y axis is directed along the unperturbed plane front. As the front propagates, its shape changes in a way that can be readily determined from the Huygens principle. Depressions are replaced by corner points. However, a corner point propagates more rapidly, its velocity being $u/\cos\alpha$, where α is the angle between the y axis and the front at this point. Propagation of the corner points compensates the increase in curvature, and the steady-state value of the amplitude is $\sim\Omega/uk^2$. Numerical calculations[125] have shown that, when $\mathrm{Le}>1$, the solution describing the combustion wave does actually reach a stationary state (uniform motion) in which the front is curved. The curvature scale is $2\pi/k_m$, and the convex portions are separated by "corner points" at which the curvature is a maximum. The temperature maximum is reached at the center of a convex portion, and exceeds T_f. Accordingly, the velocity of the curved front is higher than that of the plane front. The calculated cellular structure is thus made to resemble the observed structure.

The stabilization of curvatures by the corner points is a purely geometric factor which works equally well for diffusional and hydrodynamic instabilities. The growth rate of the latter is shown by (3.1) to increase with k. However, for large k, the dependence of the combustion rate on the front curvature[22] due to transport phenomena (as discussed above) becomes significant. Short-wave hydrodynamic modes turn out to be stable, so that the growth rate spectrum $\Omega(k)$ has a maximum for a certain k_m. This determines the scale of the structure stabilized by the corner points. According to Ref. 19, the growth of long-wave modes eventually suppresses the cellular structure. For example, during flame propagation in a tube, when the Reynolds number is sufficiently high and hydrodynamic instability should develop, the laminar flame transforms into a convex flame (single cell, covering the entire cross-section of the tube; cf. Ref. 167).

3.3. In-phase oscillations

We now turn to region II in Fig. 13. Combustion waves in condensed systems ($D\ll\chi$) belong to this case. The instability is due to the fact that the heated zone contains practically no reaction products[20] because there is little diffusion. The front can traverse the heated medium at high speed, but comes to rest after the heated layer has been consumed. The temperature in the reaction zone falls, and thereafter the influx of heat from the combustion products produces a new heated layer, and the entire picture recurs. Instead of the uniform motion of the combustion wave, a self-oscillatory state is established in which its velocity and other characteristics are periodic functions of time. Combustion waves in condensed media generally have a complicated banded structure (see Section 4). In view of the effect of this structure on diffusional instability, we can subdivide all systems into two classes. In gunpowder and other explosive media, the combustion wave is accompanied by a sharp fall in density (evaporation, gasification). During the depression stage, which follows the rapid combustion of the heated layer, the influx of heat from the gaseous zone of reaction products is relatively small and, instead of growth of oscillations, we frequently have extinction (similarly to the separation described in Section 2.2). Fuel mixtures containing condensed reaction products (thermites are an example) belong to the second class. The high thermal-energy density in the products effectively supplies the combustion front during the depression stages. Different types of self-oscillation are therefore readily observed during combustion in such systems. Some are described below.

É. I. Maksimov has observed[23] pulsations in radiation from the hot surface of nitroglycerin powder and noted the formation of condensed intermediate products on the surface, i.e., a grid of carbonized cellulose filaments. Theoretical analysis[43] of a model of gunpowder combustion that extended previous work[20] led to a solution for the in-phase oscillations of the front (excited in the hard state). Oscillations in the rate of combustion of a thermite compound were reported in an earlier paper.[126]

Systematic studies of combustion waves in mixtures containing condensed reaction products have identified the region in which oscillatory states occurred, and their properties were investigated. One of the factors that stimulated interest in these systems was the development and application of methods of self-propagating high-temperature synthesis based upon them (see Ref. 127).

Numerical experiments have played a major part in the investigation of different self-oscillatory states. In order to reach a given state, it is sufficient to choose the initial conditions in an "attractor region." Of course, whether a particular experiment is effective depends on the extent to which the chosen conditions are close enough to a particular state. The attainment of in-phase oscillations[44] was the first to be implemented. The evolution of these oscillations as the bifurcation parameter (3.2) moves into the instability region is illustrated in Fig. 15, which presents the results reported in Ref. 128. Velocity oscillations are excited in the soft state, and there is clear evidence of successive period doubling.

In-phase oscillations have been observed[24] during the combustion of many systems (Nb–B, Hf–B, and so on). Their characteristics are in good qualitative agreement with the foregoing discussion and with numerical experiments.[44,128] The quantity s in (3.2) is a decreasing function of temperature in the reaction zone [e.g., in the simplest case, $s=(1/2)(Q\varepsilon T_f^{-2})$. This means that dilution of the burning mixture with an inert material[24] (reaction product) corresponds to an increase in s. The measured frequency of the oscillations decreases with the degree of dilution. In the

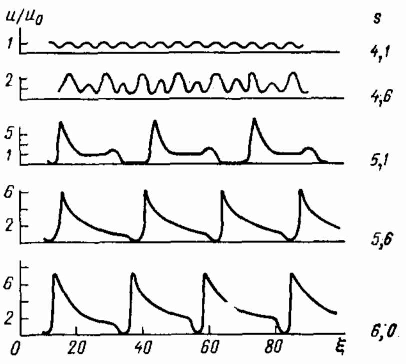

FIG. 15. Evolution of oscillations in the velocity of a combustion wave: u_0—velocity of a steady-state (unstable) front; ξ—dimensionless coordinate.

self-oscillatory state, the combustion wave propagating over the specimen produces a structure that is periodic in its chemical composition because the "depth of transformation" during crests and troughs is different.

A theory of the steady-state and self-oscillatory propagation of the "neck" produced during the deformation of a polymer rod was developed in Ref. 129 on the basis of an analogy with the combustion wave (for $\mathrm{Le} = 0$), and the corresponding experiments were reported in Ref. 130. Oscillations in the velocity of the crystallization front in a highly supercooled liquid[95] appear to be possible when the "intrinsic" velocity (2.16) of the separation boundary between the phases increases with temperature. In the oscillatory state, the liquid layer adjacent to the front becomes heated and crystallizes rapidly. The front then comes to rest, heat is transferred from the solid phase, the phase executes another "hop," and so on.

3.4. Spin states

The propagation of a luminous "reaction focus" along a helical line on the surface of a sample was observed in Ref. 24 in addition to in-phase oscillations. This process was called spin combustion.[9] Figure 16 reproduces a photograph[131] of a longitudinal cut through a sample in which this type of combustion has taken place. Since the temperature of the focus is higher than that of the main front, the helical trajectory is determined by the composition of the combustion products. Comparison of the sample diameter with the pitch of the helix shows that the linear velocity of the focus is several times greater than the velocity of the main front (the latter is of the same order as in the steady state). While in the case of in-phase oscillations, the accelerated motion of the front near the heated layer of the material occurs against the temperature gradient (as in the steady-state wave), in the case of spin, the focus runs over the heated layer along the front.

FIG. 16. Longitudinal cut through a specimen burnt in the spin state. Initial composition Ti + FeB.

These simple concepts are in agreement with numerical calculations.[25] Equations (1.1) and (1.2) with $D = 0$ were integrated over a two-dimensional domain in the form of a band of width d. The cyclic condition $T(y = 0) = T(y = d)$, $\eta(y = 0) = \eta(y = d)$ was imposed at the edges of the band, and the ignition condition (high temperature) was applied to one of the ends. When $s = 12.5$ (this corresponds to the instability region in Fig. 13), the system approaches the state of in-phase oscillations as d increases, and the spin state evolves thereafter. For still greater values of d, the structure of the "spin" waves becomes more complicated: two foci are formed and run along the helix in the same direction. The "multiplication" of foci was observed even in the early experiments.[24] Special examination[132] subsequently revealed structures with two or three foci, associated with an increase in the sample diameter (see below).

An original approach to the theory of spin states was developed in Ref. 46. A phenomenological equation was postulated for the function $\xi(y, t)$ defining the position of the front in the coordinate frame moving with the mean combustion velocity:

$$\ddot{\xi} + \omega_0^2 \xi = 2\omega_2 \left[\dot{\xi} - \frac{4}{3} (A_0 \omega_0)^{-2} \dot{\xi}^3 + l_0^2 \frac{\partial^2 \dot{\xi}}{\partial y^2} \right]; \qquad (3.3)$$

where $\omega_0^2 = \omega_1^2 + \omega_2^2$, ω_1, ω_2 are the frequency and growth rate of laminar perturbations, known from studies of the stability of a stationary combustion wave for $\mathrm{Le} = 0$ (see Section 3.1), and A_0 is the amplitude of the in-phase oscillations. According to (3.3), each segment of the front can be assigned a nonlinear oscillator. The nonlinearity ensures that the instability is stabilized. Coupling between neighboring oscillators, described by the last term in (3.3), is due to thermal conduction. The range of this coupling is equal to the correlation length l_0. While the medium is present in the reaction zone, a given portion of the front does not have time to receive heat from regions located at distances exceeding l_0.

To describe the spin states, the periodic boundary condition $\xi(y,t) = \xi(y + d,t)$ must be added to (3.3), where d is the perimeter of the sample cross section. As d increases, in addition to the in-phase oscillations, there are also solutions corresponding to spin combustion with one, two, and so on, foci. The state corresponding to spin combustion turns out to be hard, since solutions with sufficiently small amplitude are unstable. Both numerical experiments[45] and phenomenological theory[46] deal with "one-dimensional" fronts; in the case of a cylindrical sample, this means that the reaction is localized in a thin surface layer.

A systematic analysis of spin states was performed in Refs. 47 and 133 in the proximity of the stability boundary, where the solution was not too different from an unstable steady-state wave (see also Ref. 134). The corresponding corrections can be calculated from (1.1) and (1.2), linearized on a steady-state plane wave $T(x + ut)$, $\eta(x + ut)$, where, in the frame in which the steady-state wave is at rest, the coefficients of the linearized set of equations do not depend on time. A general scheme of this type of calculation is described, for example, in Ref. 71 (Section 27). The solution is a periodic function of time (frequency ω_1), with amplitude

FIG. 17. Specimen burnt in the stochastic state.[137]

$A \sim \omega_2^{1/2}$. The factors in the solution that are functions of coordinates, in turn split[134] into products $f_1(x)f_2(y,z)$, where f_2 are eigenfunctions of the Laplace operator on the cross section of the sample. In the case of a circular cylinder, it is convenient to transform[47] to the moving coordinate frame defined by $x = x' + ut$, $\varphi \equiv \arctan(z/y) = \varphi' + \omega_1 t$, in which the problem becomes a steady-state one. In general, the "two-dimensionality" of the front leads to a great variety of structures. In addition to the in-phase oscillations and spin states mentioned previously, solutions appear with periodic splitting and merging of foci, oscillations of foci between the center and the periphery, and so on.

The stability of different periodic solutions is due to the nature of the growth-rate spectrum $\omega_2(k^2)$ (Ref. 134). Suppose that the bifurcation parameter is the quantity s in (3.2), and that the stationary wave loses stability when $s = s_*$. When $\omega_2(s_*)$ vanishes for $k^2 = 0$, the in-phase oscillations are stable, but, when $k^2 > 0$, the spin states are stable. We recall that, strictly speaking, we are concerned only with the neighborhood of the point s_*. According to Ref. 119, the second case occurs for $\mathrm{Le} = 0$, and the line $s(k^2)$ corresponding to the stability boundary has a minimum for $k \sim l_0^{-1}$. However, the depth of the minimum is small. (For a given s, the short-wave modes $k \gtrsim l_0^{-1}$ are damped out by heat conduction, and this is responsible for the "basic" monotonic dependence on k of the position of the boundary. The behavior for small k is evidently dominated by the interplay of relatively weak interactions.) Because the depth of the minimum is small, we may suppose that different periodic states are "almost equivalent" in a transition from one state to another for a sufficiently small change in the parameters or the conditions of excitation as is observed experimentally.

In addition to the complication of the structure of spin states mentioned above, it has been found experimentally[135] that, in samples of rectangular cross-section, the focus hops periodically from edge to face (in accordance with the calculations reported in Ref. 134); when ignition is applied to the center of a disk, the focus moved over a discontinuous untwisting helix[136]; and so on. We have already noted that the dilution of the initial mixture with reaction products simulates an increase in s. Under these conditions, one observes a transition from a steady-state wave to in-phase oscillations, and then to spin combustion. Between the in-phase oscillations and the spin states, there is an interval of concentrations that leads to a random propagation of the front [irregular oscillations of the focus or several foci[132,137] (Fig. 17)].

We note in conclusion that, in the case of a soft (or a hard, but approaching a soft) instability development, the nature of the new attractor state is predetermined by the "eigenfrequency" on the stability boundary. For example, $\mathrm{Im}\,\Omega \neq 0$ on the boundary of region II in Fig. 13, and periodic waves (in-phase oscillations and spin states) are created. Near the boundary of region I we have $\mathrm{Im}\,\Omega = 0$, and the wave remains a steady-state one, but acquires a cellular structure.

3.5. Complication and stochastization

The region of unstable stationary waves $s > s_*$ has not as yet been penetated too far. In 1971, G. I. Barenblatt suggested that the complication of the structure of in-phase oscillations found in numerical experiments[44] (see Section 3.3) led to a stochastic combustion state ("one-dimensional thermal turbulence") as s increased further. The sequence of bifurcations, i.e., the period doubling demonstrated in Fig. 15, seems to present us with evidence for a relatively simple "scenario" of stochastization. However, numerical experiments[44,128] are artificially restricted by the one-dimensional situation, and the plane front is "secured by hand." It became clear later that the instability of the plane combustion wave generated not only in-phase oscillations, but also a multitude of non-one-dimensional periodic states, as mentioned in Section 3.4.

Investigations of nonstationary combustion in the Ti-B mixture containing Cu as the inert additive,[132] or the iron-zirconium thermite diluted with the reaction products,[137] mentioned in Section 3.4, yield the following picture. As the concentration of the inert component increases, the in-phase oscillation state becomes randomized, but the stochastic state is not one-dimensional, and irregular pulsations of one or more foci are observed. The range of concentrations corresponding to combustion in the stochastic state is restricted, and strong dilution leads to the replacement of the stochastic state by a regular state, i.e., spin combustion. This change of state is one of the most topical theoretical problems in this area.

4. MULTIZONE STRUCTURE OF PROGRESSIVE WAVES

From the hydrodynamic point of view, the combustion wave is a surface of discontinuity of density, temperature, concentration, and so on. The structure of the heated zone was taken into account in studies of separation and diffusional instability, while the reaction zone was looked upon as the surface of discontinuity of thermal and diffusion flows. To calculate the velocity of combustion waves and of the analogous progressive waves, we must now consider their structure as a whole. In many cases, the structure of a steady-state wave is complex (multizone). In a complex structure which, like a simple structure, constitutes an attractor for a whole range of initial conditions, the effects of self-organization are particularly prominent, as is the formation of that "ordering" which Schrödinger contrasted with the order in crystals[138] as far back as 1943.

Here, we shall briefly describe a few examples of the multizone structure of steady-state waves, due to different factors. Mathematically, each case requires a set of equations that is more complicated than equations (1.1) and (1.2) of Sections 1–3. Accordingly, the results which we shall now consider can be classified as belonging to the "zoological level," even more so than the previous results. In addition, it is found that a complicated wave can always be divided into a number of zones of different function, and the set of equations can be simplified in a specific manner within each such zone.

4.1. Two-zone combustion wave

In Section 2.1, we considered a combustion wave consisting of heated and reaction zones. Let us now suppose that the chemical transformation occurs in two stages: $A \to B \to C$. A stationary combustion wave is described by a self-similar solution (which is a function of $x + ut$) of a set of three equations for T, η_B, and η_C. The corresponding numerical calculations and their analysis were first reported in Ref. 48. They can be illustrated by simple qualitative considerations.[49] As shown in Section 2.1, the reaction zone occupies a narrow temperature interval $(\sim T^2/\varepsilon)$. We shall start with a structure in which the first reaction occurs near the temperature T_1 and the second near the higher temperature T_2. (When $T > T_1$, the first reaction does not proceed because the original mixture A has already been consumed.) For each of the reaction zones, we can write down relationships such as (2.11), while outside these zones, the flux of heat is a linear function of temperature (Michelson's law). As far as the "internal" solutions are concerned, we follow Ref. 5 and replace (2.14) with

$$(Q_i u + q_i)^2 - q_i^2 \approx Q_i \chi F_i e^{-\varepsilon_i/T_i} \qquad (i = 1,\ 2), \qquad (4.1)$$

where $q_i = \chi T'(T = T_i + 0)$. It is assumed in (4.1) that integration of the complete set of equations leads to an analogous relationship between T_i and u, and the only difference is that there is a weak (power-type) dependence of F_i on T_i.

If we neglect heat losses, we have $T_2 = T_0 + Q_1 + Q_2$, $q_2 = 0$. The wave velocity u is then determined from (4.1) for $i = 2$, i.e., it depends only on the kinetic parameters of the second reaction. Substituting this value of u in (4.1) for $i = 1$, and recalling that

$$q_1 = u\,(T_1 - T_0 - Q_1), \qquad (4.2)$$

we obtain T_1 and hence the structure of the wave. Thus, the velocities of the two zones become equal (steady-state wave) because the second reaction zone heats the first and raises its velocity. This is the "control state." It is possible only for a limited range of parameter values for which $T_{10} < T_1 < T_2$, where $T_{10} = T_0 + Q_1$. When $T_1 = T_{10}$, the first zone can no longer be controlled and a transition to the separation state takes place. In this state,[10] the second zone has no influence on the first, $q_1 = 0$, and the wave velocity u is determined by the rate of the first reaction at its "own" temperature T_{10}. On the other hand, when $T_1 = T_2$, the two zones merge and the combustion wave degenerates to the single-zone situation. This is illustrated in Fig. 18.

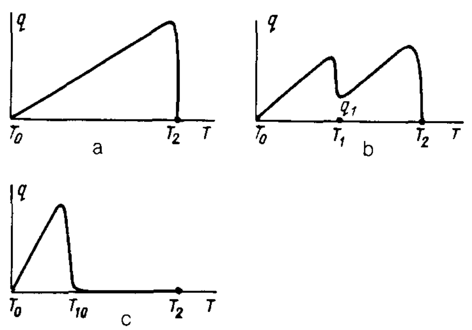

FIG. 18. Phase trajectories of the two-zone combustion wave: a—merging state; b—control state; c—separation state.

The peculiar two-zone thermal wave is generated by supplying to the separation boundary between a solid transparent dielectric and a conducting melt a sufficient amount of microwave power through the dielectric.[141] The absorbing boundary of the melt moves in the opposite direction to that of the microwaves (see Section 2.4), and heat is released in the skin layer of the melt and in the heated layer of the solid phase near the boundary. Although the conductivity of the solid phase at the melting point is usually lower by several orders of magnitude[76] than the conductivity of the melt, the power dissipated in these two zones can be comparable if the former zone is much wider than the latter. The control state prevails so long as the supply of heat from the melt to the solid continues. However, when $Qu = q_+$, where Q is the latent heat of melting and q_+ is the flow of heat from the melt to the interphase boundary, the first zone "separates," the width of the heated zone in the solid increases, and the microwaves penetrate the entire melt.

When $Q_2 < 0$, the control state is not possible.[142,143] Instead, there is bistability: depending on the ignition conditions, we can have either the merging state (the temperature in the wave increases monotonically from T_0 to $T_2 < T_{10}$) or the separation state (the temperature increases to almost T_{10} and this is followed by a fall to T_2 due to the slow second reaction). It is clear that the wave velocity in the separation state is greater in such systems than in the merging state.

4.2. Multizone waves

The idea of three propagation states of the two-zone wave (control, merging, and separation) can be naturally transferred to multizone structures.[49] According to these ideas, the space of the parameters (pressure, initial temperature, and so on) splits into regions in each of which the wave velocity depends on the kinetic constants (activation energy, pre-exponential factor) of only one reaction. There is always a dominant zone in the wave structure, but, as the parameters vary, this function can be transferred from one zone to another.

However, in real multizone waves, there are not only reactions, but also phase transitions and other processes that result, in particular, in the evolution of different inhomogeneities. The picture is significantly complicated by the interrelation between the reactions and these processes. Figure 19 shows the temperature distribution in a steady-state combustion wave in the alloy 5Ti + 3Si, measured with microthermocouples compacted into the samples.[144] Judging by this profile, the structure of this wave is an example of the complication mentioned above.

4.3. Wide zones

In the simplest case, the influence of the inhomogeneity of the medium reduces to a significant widening of the reaction zone. As noted in Section 2.1, the narrow width of the reaction zone is due to the activation-type (Arrhenius) dependence $\Phi \sim \exp(-\varepsilon/T)$. This ensures that the reaction zone occupies the temperature interval $T_{\rm f}^2 \varepsilon^{-1} \ll Q$. However, diffusion restrictions lead to a weaker temperature de-

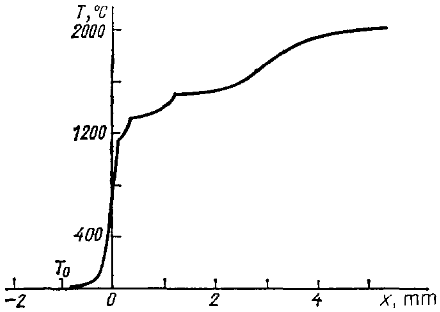

FIG. 19. Temperature profile of a combustion wave in the mixture 5Ti + 3Si. Titanium particle size ≥45 μm.

pendence of the reaction rate at high temperatures (see Section 1.5).

Since, in a combustion wave, the heat can be transferred only to distances $l_0 \sim \chi/u$, a wide reaction zone is found to consist of two zones[145] whose structure and functions are different. In the propagation zone, whose width is $\sim l_0$, practically the entire released heat is transferred to the fresh mixture. It follows that the temperature does not change very much within this zone. In the remaining part of the reaction zone (burnout completion zone), the heat flow in the direction of propagation of the wave can be neglected and practically the entire heat released in a given portion of the medium is expended in heating this portion. In its heat-flow distribution, a wave with a wide reaction zone resembles a two-zone wave in the separation state (see Fig. 18c). The relatively small temperature range within the propagation zone means that this zone can be approximately characterized by a single temperature T_*, which now plays the same part as $T_{\rm r}$ in the case of a wave with a narrow reaction zone. The wave velocity u can still be estimated from (2.6) provided we introduce the replacements $T_{\rm r} \to T_*$, $\Gamma \to 1$. A calculation of u for a given function $\Phi(\eta, T)$ is given in Ref. 145.

4.4. Gasification

In gunpowder and certain other condensed media, the reaction products are gaseous and a phase transition occurs within the structure of the combustion wave. It was assumed in early work[20,146] that the condensed medium first evaporated and then reacted, releasing heat which was transferred to the surface of the specimen and produced evaporation. Subsequent experiments showed[147] that a substantial fraction of the heat was released in the surface layer of the condensed material. Systems in which the surface layer is solid or porous are discussed in Ref. 148. Gaseous reaction products are extracted through the pores of the "burning" surface. The solid carcass of the surface layer can be destroyed by reactions and gas jets, and this explains the dispersion of this layer observed[147] at low pressures.

In most gunpowders, the heated surface layer is in a liquid state. Equilibrium release of the gas produced in the reaction should give rise to the foaming of this layer and, even for small values of the transformation depth η, the density should fall sharply. Calculations based on the equilibrium gas-release model[149] have shown that, at moderate pressures, the reaction zone in the surface layer (K zone) is controlled by the reaction zone in the dispersed medium above the surface (D zone). According to the data presented in Ref. 147, the K-zone plays the leading part (mechanical removal of the D-zone does not lead to extinction), which corresponds to the separation state.

It has been suggested[150] that equilibrium gas release does not actually occur and that the gas concentration in the K-zone is significantly higher than the solubility η_0 (usually, $\eta_0 \ll 1$). The resulting gas is removed by diffusion through the burning surface well before the supersaturated solution decays. Because the diffusion coefficient in the condensed material is low, the first term in (2.2) need not be taken into account when the structure of the combustion wave is calculated, except for the neighborhood of the interphase boundary (burning surface). The boundary conditions on the surface are

$$\eta \approx \eta_0, \quad \rho_s u \eta_0 - \rho_s D \eta' |_0 = \rho u_g; \tag{4.3}$$

where ρ_s and ρ are the densities of the condensed material and of the gas, respectively, and $\eta'|_0$ is the gradient on the surface on the side of the K-zone. The rate of outflow of gas from the surface, u_g, is determined by the condition $\rho_s u \eta_s = \rho u_g$, where η_s is the depth of transformation in the K-zone. It follows from (4.3) and (2.2) that a narrow diffusion zone between the K-zone and the surface is present, and its width $\sim D/u$ is small in comparison with the width $\sim \Gamma\chi/u$ of the K-zone. The chemical source in (2.2) can be neglected within the diffusion zone, and the concentration of products falls from η_s to η_0 in proportion to $\exp(ux/D)$. In the laboratory frame, the initial material in front of the combustion zone is stationary, whereas the portion of this material contained within the diffusion zone moves together with the wave.

The nonmonotonic distribution $\eta(x)$ is analogous to the "inverted" temperature distribution in the laser evaporation wave.[151] The light flux incident on the surface of a condensed material is absorbed in a layer of width $\sim \varkappa^{-1}$. Since the surface is a heat sink, the temperature distribution in the condensed phase has a maximum at a distance $\sim \chi/u$ from the surface, where u is the evaporation velocity, i.e., the velocity of the interphase boundary. It is shown in Ref. 151 that a plane interphase boundary is unstable in the case of the "inverted profile." A similar instability apparently occurs in the case of the combustion wave with a diffusion zone.[150] The origin of the instability can be explained as follows. The velocity of the hot surface (in the laboratory frame) is proportional, according to (4.3), to the diffusion current and, consequently, inversely proportional to the width of the diffusion zone. When a depression is formed on the surface, the width of the diffusion zone is reduced, and the velocity of the surface increases, so that the depression becomes deeper, and so on.

4.5. Filtration waves

Motion in the porous medium of the reaction zone between the solid carcass and the gas is accompanied by filtration of the latter. This problem was first examined in relation to adsorption in Ref. 170 (p. 62). At constant filtration velocity v, the boundary between the "pure" and saturated regions of the sorbent moves uniformly with velocity u given by

$$u n_0 = (v - u) n_1,$$

where n_0 is the number of particles saturating a unit volume of the porous medium and n is the concentration in the original flow. During the filtration of a mixture, the difference between the velocities of adsorption waves corresponding to the mixture components gives rise to separation (this is the basis of chromatography). In the case of chemical interactions that result in the formation of a solid product, the initial experimental[152] and theoretical[153] work was followed by detailed studies of the structure and characteristics of filtration waves under different conditions ("natural" filtration, in which the pressure gradient is produced not by external conditions, but by the consumption of the gas in the reaction zone; or the gas is drawn through the porous specimen by an applied constant head of pressure, or by consumption of gas along or against the propagating filtration wave). States of incomplete transformation, wave front reversal, wave front division, and other effects are found to occur, depending on the ratio of the characteristic relaxation and filtration times.

We must now consider the case of "associated filtration," in which the gas enters the reaction zone through a layer of reaction products. It is shown in Ref. 52 that the temperature distribution in a porous medium depends on the concentration of the reacting component in the gas flow. The first integral of the steady-state one-dimensional equation of thermal conduction is

$$\chi T' + Qu\eta = [u - \rho m v \rho_s^{-1} (1-m)^{-1}] (T - T_0) \tag{4.4}$$

[compare this with (2.1) and (2.2)], where m is the porosity (fraction of the volume associated with the pores), v is the absolute velocity of the gas flow, and ρ_s is the density of the pore-free solid material. For simplicity, we are assuming that the specific heats of all the media are equal and the reaction does not alter the porosity or density of the solid carcass. The combustion wave velocity u is given by the obvious relation

$$\rho_s (1 - m) u = \rho m v a, \tag{4.5}$$

where a is a dimensionless coefficient that depends on the stoichiometric ratios and the concentration of the reacting component in the gas. To the right of the reaction zone, we have $\eta = 1$ and the temperature

$$T = T_0 + Q (1 - a^{-1})^{-1} \tag{4.6}$$

is higher than that in the thermally insulated burnt-out mixture. The point is that the incident gas flow (original temperature T_0) cools the burnt-out layer and transfers heat to the "temperature plateau" (4.6). The width of this plateau is in the ratio of $1 - a^{-1}$ to the width of the burnt-out layer.

When $a < 1$, the expression given by (4.6) becomes meaningless, and the structure of the filtration wave in this region is significantly different. Convective heat transfer is then so high that the high-temperature plateau lies ahead of the reaction zone. At the rear of this zone, where $\eta = 1$, we have $T = T_0$. The combustion-wave structure is thus "inverted."[52] The constant in (4.4) was chosen in accordance with the condition $\eta = 0$, $T = T_0$. In the case of the inverted structure, the right-hand side of (4.4) acquires the additional term $-Qu$ and the temperature ahead of the reaction zone is

$$T = T_0 + Q (a^{-1} - 1)^{-1}. \tag{4.7}$$

In the inverted combustion wave, we have not an increase but a fall in temperature, chemical transformation does not occur in the hot medium ahead of the wave, and the medium receives only the inert component of the gas flow since the active component is completely consumed in the reaction zone. It is clear from (4.7) that, when a is suitably chosen (i.e., the gas composition is right), associated filtration will efficiently heat up the initial solid medium even when the heat of the reaction is small (depleted oil deposits, and so on). As in the case where $a > 1$, the width of the hot region increases with time.

4.6. Melting of porous material

Analyses[52,153] of filtration waves have been based on the assumption that the temperatures of the two phases (solid and gas) were equal in every small portion of the medium. This assumption is valid only when the wave velocity is not too high, so that the medium spends sufficient time in the wave for heat to be transferred over distances of the order of the inhomogeneity length d (the pore diameter and the separation between pores are usually of the same order). Studies of melting waves in porous media[53] have shown that interphase heat transfer has a dominant influence on the characteristics of these waves.

The motion of the boundary between metastable and equilibrium phases is examined in Sections 2.2 and 2.5. Here, we shall consider melting due to heat release in the melt. The source of heat may be a reaction occurring only in the liquid phase, or a flowing current when the solid phase is dielectric and the melt is a metal. Melting of dielectrics by heat transfer from hf-heated melt is described in Ref. 77. When the solid material is a porous medium (for example, powder), the solid particles are heated by the melt flowing through the pores. This flow occurs because a liquid always wets its own solid. The variables characterizing this type of flow can be used to form the grouping

$$d\mu\nu^{-1} = \chi_{\text{eff}}, \tag{4.8}$$

which has the dimensions of thermal diffusivity (μ is the surface tension and ν the viscosity) and its magnitude exceeds the usual value of χ by several orders of magnitude. The motion of the reacting melt into the interior of the porous medium is equivalent to the transport of the source of heat. The melting wave, i.e., the two-phase regions (the pores are filled with the liquid) between the solid phase and the melt, cannot be subdivided into heat-release and heated zones, whereas all the solitary thermal waves considered previously can be so separated. The thermal structure of the melting wave is fundamentally "two-dimensional": in addition to the direction of propagation (along the normal to the macroscopic powder-melt boundary), there is a "direction" of microtransfer of heat along which the heat flows from the melt to *each* solid particle.

This microtransfer is due to ordinary thermal conduction. However, the surface area of interphase contact (and, together with it, the rate of heat transfer) is greater by a factor of ld^{-1} than the contact area between the melt and the monolithic (pore-free) solid material, where

$$l \sim \chi_{\text{eff}} u^{-1} \tag{4.9}$$

is the depth of penetration of the melt into the pores. Similarly, in the course of turbulent burning, the mixing of the hot particles of burnt-out gas with the cold initial mixture increases the effective surface area of the flame and, hence, an increase in the rate of burning.

Crystallization of the liquid rather than melting of the solid occurs on the leading edge of the two-phase region. The leading edge of the flowing melt constantly comes into contact with new solid particles at initial temperature T_0. The influx of heat into each such particle is high (initially, infinite). This means that, whatever is the temperature of the melt on the leading edge, the heat arriving on the surface of the solid particles cannot replace the heat expended in heating these particles, so that the melt begins to "freeze on" to them. The latent heat of crystallization that is released as a result of this is expended in heating up the particles. As this heating continues, the rate of interphase heat transfer is reduced, so that, at a certain distance from the leading edge, the heat released is in balance with the heat lost to the solid phase. The direction of the phase transition is reversed, and melting begins.

The porosity $m(x)$ in the two-phase region is thus a nonmonotonic function and has a minimum at a certain x_*. Partial crystallization for $0 < x < x_*$ reduces the fraction of material in the liquid state, and weakens the source of heat. This means that the thermal output of the source has a threshold for the steady-state propagation of the melting wave.

The threshold power density is

$$F_t = 4\varkappa_s (m_0 d)^{-2} (1 - m_0\chi)(T_e - T_0)^2 (T_e - T_0 + Q)^{-1}, \tag{4.10}$$

where $\varkappa_s$ is the thermal conductivity of the solid phase, m_0 is the initial porosity, T_e is the melting point, and Q the latent heat of melting. At the threshold power, the minimum value is $m(x_*) \neq 0$, and the presence of the threshold is a consequence not of the stopping up of the pores but of separation, similarly to the phenomena described in Sections 2.2–2.5.

Figure 20 shows schematically the two-dimensional distribution of current lines in the coordinate frame in which the wave is at rest in the case of the "sandwich model" (flat plates of the solid phase in front of the two-phase region, separated by gaps, i.e., pores). Some of the lines form closed loops, i.e., the trapped portion of the material travels together with the melting wave. The trapped material periodically changes its state: it crystallizes on the leading edge of the wave and then, as the wavefront passes, the material melts, flows toward the leading edge, recrystallizes again, and so on.

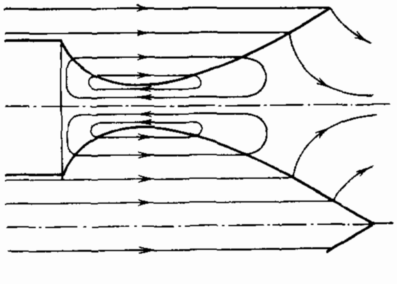

FIG. 20. Current lines in the "sandwich model": thick lines represent the phase separation boundary.

When $F > F_t$, the large value of χ_{eff} leads to a high wave velocity, in accordance with (2.6). When the thermal power is below the threshold value, the melt penetrating the pores freezes up, forming a solid layer between the porous charge and the melt. This layer melts slowly as a result of thermal conduction. When the melt is again in contact with the porous medium, it rapidly penetrates it, forming a new frozen layer, and so on. The process is quasiperiodic, and the mean wave velocity in this state is determined by the slow melting of the frozen layers. The velocity is lower by a factor of about $(\chi_{\text{eff}}/\chi)^{1/2}$ than the velocity in the steady state.

4.7. Thermal wave in a flow of helium

Filtration of a liquid can be accompanied by considerable release of heat as a result of friction. Some aspects of the hydrodynamic thermal instability were examined in Section 1.5 where the viscosity was assumed to be a decreasing function of temperature, which is typical for most liquids. There are, however, cases where the viscosity increases with temperature in a certain range (examples include sulfur, where the increase is due to irreversible structural changes at $T \sim 450$ K). The increase in viscosity gives rise to an N-shaped relationship between the head of pressure and the rate of flow in the case of Poiseuille flow. Actually, $v \sim P\nu^{-1}$. When the head of pressure P is small, the dissipative heating of the liquid is small, and $\nu \simeq$ const. However, as P increases, both temperature and viscosity increase. This means that the $v(P)$ curve has a negative slope for a certain range of values of P. This region of the characteristic is unstable (see Section 1.6), the flow becomes inhomogeneous, and a thermal "domain" is formed and is transported by the flow. The velocity v does not depend on P and is determined by the condition of equilibrium between the kinetic "phases" (cold and hot liquid), by analogy with (1.25) and (1.28). As the domain leaves the end of the tube, the hydrodynamic resistance falls and the velocity increases. Instability then ensures that a new domain is formed. The flow rate thus pulsates with a frequency $\omega \sim vL^{-1}$, where L is the tube length.[154] The entire phenomenon is the hydrodynamic analog of the Gunn effect (see, for example, Ref. 83).

In an ordinary liquid, the velocity of a thermal domain is trivially equal to the flow velocity. In liquid helium, on the other hand, which flows in a capillary in a thermostat held at a temperature $T_0 < T_\lambda$, the kinetic phases are He I and He II. They are "kinetic" only in the sense that they have different temperatures, and heat flows into He II through the interphase boundary. Since heat transfer in He II is due to the flow of the normal component, wide convective zones are formed on either side of the thermal domain (He I region). In one of these zones, which lies in the lower flow, the direction of the normal velocity is the same as the direction of the resultant flow, whereas these directions are opposite in the zone lying in the upper flow. In the latter case, solutions describing flow in the convective zone and in He I obviously cannot be directly joined across the interphase boundary. It is shown in Ref. 51 that there is a narrow boundary zone between the convective zone and the He I region, in which molecular heat transfer is significant. This structure corresponds to a nonmonotonic pressure distribution in the capillary.

According to Ref. 51, the interphase boundary in helium flow is always moving relative to the liquid, and this is accompanied by the growth of the phase in the upper flow. If we consider a capillary containing a thermal domain, the He I → He II transformation occurs on the "upper" boundary of the domain and the reverse transition occurs on the "lower" boundary. When the rate of flow is small, the upper boundary moves relative to the liquid more rapidly than the lower boundary, and the He I region disappears. When the rate of flow is high enough, He I fills the entire capillary. Equal velocities of the two interphase boundaries correspond to a particular flow rate v_0. It is precisely this value that is established[154] when the head of pressure P is applied. Actually, when $v < v_0$, the length of the He I region is reduced and the hydrodynamic resistance falls, which leads to an increase in the flow rate, and so on. Within the plateau, on which the domain is stable, the motion of the domain does not reduce to a simple drift, and the domain velocity is greater than the flow velocity v_0.

CONCLUSION

In the 1920s, attention was riveted to atomic phenomena, and quantum mechanics was created. Against this dazzling background, advances in other areas (e.g., self-oscillations or chain reactions) appeared to be relatively less striking. Today, nonlinearity is the most popular topic among theoreticians, especially, of course, under the guise of nonlinear gauge theory. Kinetics has naturally assumed a more modest role but, even there, we see a considerable level of activity.[11] A multitude of processes has been investigated, and relationships between different effects have been established in many cases. Whenever possible, we have tried to concentrate our attention on connections of this type. However, universality is hardly easier to achieve in kinetics than it is in field theory.

Publications devoted to particular processes (and they constitute the great majority of theoretical papers on kinetics) at best mention analogies that constitute the origin of phrases such as "light combustion," "kinetic phases," and so on. In this situation, any attempt at a generalization is particularly valuable. The greatest efforts in this direction have been made by mathematicians, or by people approaching the subject from the mathematical point of view. There is obvious value in such work, and significant advances have been made. On the other hand, since the interests of mathematicians and physicists are not always identical, the reaction to this has been a tendency toward less refined ideas and concepts. The reader is now in a position to judge the outcome of all this. We recognize ourselves that the net result has been a regrouping of a limited volume of factual information, and there is no point as of now in claiming that anything more than that has been achieved. At any rate, it appears that a long and difficult path lies ahead.

The sphere of macrokinetic investigations is continuously expanding. Laser thermochemistry[155,156] is one of the most recent achievements. Its particular feature is that optical heating is almost instantaneous and that absorptive power is a nonlinear function of temperature and chemical composition. The role of thermal fluctuations in chemical kinetics has begun to be investigated.[159,171–173] It has been shown[171–173] that, in the concluding stages of the reaction, when the concentration of the initial material is low, spatial inhomogeneities due to fluctuations transform the reaction to the diffusion state. This alters the asymptotic behavior of $\eta(t)$ as $t \to \infty$. There is a known similarity between the equations for chain reactions and the so-called population dynamics,[157] although the consequences of this similarity have not as yet been adequately explored. Moreover, experience accumulated by studying relatively simple nonlinear kinetic systems should be useful to those who are bold enough to tackle ecological problems for which so far there are only "philological" solutions. We end with Feynman's optimistic words (retranslated from the Russian, so may be not a literally exact quotation): "Because they are unaware of the possibilities of simple equations, people frequently conclude that to explain all the complexity of the world we need something God-given and not simply equations."

[1] For typical reactions, $\varepsilon \gg T$ throughout the temperature range that we are considering (in which chemical compounds exist).

[2] We note the early work reported in Ref. 158 on thermal explosions and flame propagation, which was ahead of its time. Unfortunately, it was rapidly forgotten (in contrast to Ref. 1, it was not based on chemical kinetics).

[3] Quasistationary concentrations are assumed for other reactions.

[4] Theoretical studies of the late stages of explosive instability are not adequately advanced in many cases. It is known that shock and detonation waves (in chemical systems), the formation of streamers during breakdown, and so on, are all possible during the late stages.

[5] Or in a system interacting with a thermostat.

[6] Processes involved in the establishment of an inhomogeneous state in a barretter are examined in Ref. 162.

[7] We note that A. S. Kompaneets estimated the velocity of a nerve impulse, assuming that the influence of the reduction stage of this quantity was unimportant.[67]

[8] Actually, the calculated function RE $\Omega(k)$ is nonmonotonic. A weak maximum[43,119] occurs for $k \neq 0$.

[9] This terminology is introduced by analogy with spin detonation investigated earlier; see, for example, Refs. 168 and 169.

[10] The mechanism of the transition to the separation state was originally investigated in Refs. 139 and 140.

[11] In particular, practically any issue of Phys. Rev. Lett. contains papers on strange attractors.

---

[1] N. N. Semenoff, Z. Phys. **48**, 571 (1928).
[2] D. A. Frank-Kamenetskiĭ, Zh. Tekh. Fiz. **9**, 1457 (1939).
[3] Ya. B. Zel'dovich, Zh. Tekh. Fiz. **11**, 493 (1941).
[4] Ya. B. Zel'dovich and D. A. Frank-Kamenetskiĭ, Zh. Fiz. Khim. **12**, 100 (1938).
[5] D. A. Frank-Kamenetskiĭ, Diffusion and Heat Transfer in Chemical Kinetics (in Russian), Academy of Sciences of the USSR, Nauka, M., 1967.
[6] First All-Union Symposium on Macroscopic Kinetics and Chemical Gas Dynamics: Abstracts of Papers (in Russian), Joint Institute of Chemical Physics, Academy of Sciences of the USSR, Chernogolovka, 1984.
[7] L. D. Inge, N. N. Semenoff, and A. F. Walther, Z. Phys. **32**, 373 (1925).
[8] S. A. Bostandzhiyan, A. G. Merzhanov, and S. I. Khudyaev, Zh. Prikl. Mekh. Tekh. Fiz. No. 5, 45 (1965) [J. Appl. Mech. Tech. Phys. (USSR) No. 5 (1965)].
[9] A. G. Merzhanov, A. P. Posetsel'skiĭ, A. M. Stolin, and A. S. Shteĭnberg, Dokl. Akad. Nauk SSSR 210, 52 (1973) [Sov. Phys. Dokl. **18**, 298 (1973)].
[10] E. P. Velikhov and A. M. Dykhne, Proc. Seventh Symposium on Ionization Phenomena in Gases (in Russian), Belgrade, 1965, p. 47.
[11] Yu. P. Raĭzer, Laser Spark and the Propagation of Discharges (in Russian), Nauka, M., 1973 [Engl. Transl., Laser-induced Discharge Phenomena, Consultants Bureau, N. Y., 1977].
[12] D. A. Frank-Kamenetskiĭ, Second All-Union Symposium on Combustion and Explosion: Abstracts of Papers (in Russian), Joint Institute for Chemical Physics, Academy of Sciences of the USSR, Chernogolovka, 1969, p. 3.
[13] A. G. Merzhanov and E. N. Rumanov, Combustion and Explosion (in Russian), Nauka, M., 1977, p. 149.
[14] A. G. Merzhanov and E. N. Rumanov, Combustion Without Fuel (in Russian), Znanie, M., 1978.
[15] D. A. Frank-Kamenetskiĭ and I. E. Sal'nikov, Zh. Fiz. Khim. **17**, 79 (1943).
[16] D. A. Vaganov, N. M. Samoilenko, and V. G. Abramov, Chem. Eng. Sci. **33**, 1133 (1978).

[17] L. D. Landau, Zh. Eksp. Teor. Fiz. **14**, 240 (1944).

[18] G. Darrieus, J. Phys. Chim. **88**, 641 (1944).

[19] Ya. B. Zel'dovich, "Structure and stability of a stationary laminar flame at moderately high Reynold's numbers" (in Russian), Preprint OIKhF AN SSSR, Chernogolovka, 1979.

[20] Ya. B. Zel'dovich, Zh. Eksp. Teor. Fiz. **12**, 498 (1942).

[21] Ya. B. Zel'dovich, Theory of Combustion and Detonation of Gases (in Russian), Izd-vo AN SSSR, M.-L., 1944.

[22] G. H. Markstein, J. Chem. Phys. **17**, 428 (1949).

[23] E. I. Maksimov, Zh. Fiz. Khim. **37**, 1129 (1963).

[24] A. G. Merzhanov, A. K. Filonenko, and I. P. Borovinskaya, Dokl. Akad. Nauk SSSR **208**, 892 (1973) [Dokl. Phys. Chem. **208**, 122 (1973)].

[25] A. M. Zhabotinskiĭ, Concentration Self-Oscillations (in Russian), Nauka, M., 1974.

[26] V. F. Pastushenko, V. S. Markin, and Yu. A. Chizmadzhev, Usp. Fiz. Nauk **123**, 289 (1977) [Sov. Phys. Usp. **20**, 836 (1977)].

[27] V. A. Vasil'ev, Yu. M. Romanovskiĭ, and V. G. Yakhno, Usp. Fiz. Nauk **128**, 625 (1979) [Sov. Phys. Usp. **22**, 615 (1979)].

[28] V. I. Krinskiĭ and A. M. Zhabotinskiĭ, Autowave Processes in Systems with Diffusion (in Russian), IPF AN SSSR, Gor'kiĭ, 1981, p. 6.

[29] P. Glansdorff and I. Prigogine, *Thermodynamic Theory of Structure, Stability and Fluctuations*, Wiley, N. Y., 1971 [Russ. transl., Mir, M., 1973].

[30] G. Nikolis and I. Prigogine, *Self-Organization in Nonequilibrium Systems*, Wiley, N. Y., 1977 [Russ. transl., Mir, M., 1979].

[31] G. Haken, *Synergetics*, Springer, Berlin, 1978 [Russ. transl., Mir, M., 1980].

[32] R. Thom, *Structural Stability and Morphogenesis*, Benjamin, Reading, Mass., 1975.

[33] A. V. Gaponov-Grekhov and M. I. Rabinovich, Usp. Fiz. Nauk **128**, 579 (1979) [Sov. Phys. Usp. **22**, 590 (1979)].

[34] B. S. Kerner and V. V. Osipov, Zh. Eksp. Teor. Fiz. **79**, 2218 (1980) [Sov. Phys. JETP **52**, 1122 (1980)].

[35] B. S. Kerner and V. V. Osipov, Zh. Eksp. Teor. Fiz. **83**, 2201 (1982) [Sov. Phys. JETP **56**, 1275 (1982)].

[36] B. S. Kerner and V. V. Osipov, Dokl. Akad. Nauk SSSR **270**, 1104 (1983) [Sov. Phys. Dokl. **28**, 482 (1983)].

[37] E. A. Shtessel', Heat and Mass Transfer and Combustion Processes (in Russian), Joint Institute for Chemical Physics, Academy of Sciences of the USSR, Chernogolovka, 1980, p. 88.

[38] D. A. Baganov, Zh. Prikl. Mekh. Tekh. Fiz. No. 1, 114 (1977) [J. Appl. Mech. Tech. Phys. (USSR) No. 1 (1977)].

[39] A. N. Dremin, Fiz. Gor. Vzryva **19**, No. 4, 159 (1983).

[40] A. G. Kolmogorov, I. G. Petrovskiĭ, and N. S. Piskunov, Byull. MGU Ser. A No. 16, 1 (1937).

[41] R. A. Fisher, Ann. Eugenics **7**, 355 (1937).

[42] B. B. Kadomtsev, Collective Phenomena in Plasmas (in Russian), Nauka, M., 1976, p. 105.

[43] B. V. Novozhilov, Nonstationary Combustion of Solid Rocket Fuel (in Russian), Nauka, M., 1973).

[44] K. G. Shkadinskiĭ, B. I. Khaikin, and A. G. Merzhanov, Fiz. Gor. Vzryva 7, No. 1, 19 (1971).

[45] T. P. Ivleva, A. G. Merzhanov, and K. G. Shkadinskiĭ, Dokl. Akad. Nauk SSSR **239**, 1086 (1978) [Sov. Phys. Dokl. **23**, 255 (1978)].

[46] A. P. Aldushin, Ya. B. Zel'dovich, and B. A. Malomed, *ibid.* **251**, 1102 (1980) [Sov. Phys. Dokl. **25**, 273 (1980)].

[47] V. A.Vol'pert, A. I. Vol'pert, and A. G. Merzhanov, *ibid.* **262**, 642 (1982) [Dokl. Phys. Chem. **262** (1982)].

[48] B. I. Khaĭkin, A. K. Filonenko, and S. I. Khudyaev, Fiz. Gor. Vzryva **4**, No. 4, 591 (1968).

[49] A. G. Merzhanov, E. I. Rumanov, and B. I. Khaĭkin, Zh. Prikl. Mekh. Tekh. Fiz. No. 6, 99 (1972) [J. Appl. Mech. Tech. Phys. (USSR) No. 6 (1972)].

[50] A. P. Aldushin and A. G. Merzhanov, Dokl. Akad. Nauk SSSR **236**, 1133 (1977) [Dokl. Phys. Chem. **236** (1977)].

[51] E. N. Rumanov, Zh. Eksp. Teor. Fiz. **74**, 1422 (1978) [Sov. Phys. JETP **47**, 744 (1978)].

[52] A. P. Aldushin and B. S. Seplyarskiĭ, Dokl. Akad. Nauk SSSR **249**, 585 (1979) [Sov. Phys. Dokl. **24**, 928 (1979)].

[53] E. N. Rumanov, "Melting waves in a porous medium" (in Russian), Preprint OIKhF AN SSSR, Chernogolovka, 1982.

[54] B. Lewis and G. Von Elbe, *Combustion, Flames and Explosions of Gases*, Academic Press, 1961 [Russ. transl., Mir, M., 1968, p. 34].

[55] C. N. Hinshelwood and H. W. Thompson, Proc. R. Soc. (London) Ser. A **5**, 122 (1929).

[56] D. N. Kopp, A. A. Kowalsky, A. B. Sagulin, and N. N. Semenov, Z. Phys. Chem. **6**, 307 (1930).

[57] N. N. Semenov, Vestn. Akad. Nauk SSSR No. 8, 34 (1968).

[58] A. D. Margolin and A. B. Shmelev, Fiz. Gor. Vzryva **14**, No. 1, 52 (1978).

[59] N. S. Lidorenko and A. V. Sidyakin, Dokl. Akad. Nauk SSSR **202**, 566 (1972) [Sov. Phys. Dokl. **17**, 69 (1972)].

[60] A. Halbach, Arch. Elektr. **21**, 535 (1929).

[61] K. W. Wagner, J. IEE **41**, 1034 (1922).

[62] L. V. Keldysh, Zh. Eksp. Teor. Fiz. **37**, 713 (1959) [Sov. Phys. JETP **10**, 509 (1960)].

[63] L. V. Keldysh, Zh. Eksp. Teor.Fiz. **48**, 1692 (1965) [Sov. Phys. JETP **21**, 1135 (1965)].

[64] É. D. Lozanskiĭ and O. V. Firsov, Theory of the Spark (in Russian), Atomizdat, M., 1975, Chap. 4.

[65] N. M. Emanuel and D. G. Knorre, *Chemical Kinetics* (*Homogeneous Reactions*), Halsted Press, 1973 [Russ. transl., Vysshaya shkola, M., 1974, p. 333].

[66] A. G. Merzhanov and F. I. Dubovitskiĭ, Zh. Fiz. Khim. **34**, 2235 (1960).

[67] A. C. Kompaneets and V. Ts. Gurovich, Biofizika **11**, 913 (1966).

[68] A. G. Merzhanov, V. V. Barzykin, and V. T. Gontkovskaya, Dokl. Akad. Nauk SSSR **148**, 380 (1963) [Dokl. Phys. Chem. **148**, 581 (1963)].

[69] N. V. Zmitrenko, S. P. Kurdyumov, A. P. Mikhaĭlov, and A. A. Samarskiĭ, Pis'ma Zh. Eksp. Teor. Fiz. **26**, 620 (1977) [JETP Lett. **26**, 469 (1977)].

[70] A. G. Merzhanov, V. G. Abramov, and V. I. Gontkovskaya, Dokl. Akad. Nauk SSSR **148**, 156 (1963) [Dokl. Phys. Chem. **148**, 29 (1963)].

[71] L. D. Landau and E. M. Lifshitz, *Fluid Mechanics*, Pergamon, Oxford, 1959 [Russ. original, Gostekhizdat, M., 1954].

[72] A. G. Merzhanov, A. P. Aldushin, and S. G. Kasparyan, Heat and Mass Transfer (in Russian), Minsk, 1980, Vol. 3, p. 84.

[73] A. G. Merzhanov and A. M. Stolin, Zh. Prikl. Mekh. Tekh. Fiz. No. 1, p. 65 (1974) [J. Appl. Mech. Tech. Phys. (USSR) No. 1 (1974)].

[74] R. A. Pearson, Y. T. Shah, and E. S. A. Viera, Chem. Eng. Sci. **11**, 2079 (1973).

[75] Ya. B. Zel'dovich and S. B. Pikel'ner, Zh. Eksp. Teor. Fiz. **56**, 310 (1969) [Sov. Phys. JETP **29**, 170 (1969)].

[76] L. V. Keldysh, Vestn. Akad. Nauk SSSR No. 4, 35 (1964).

[77] V. I. Aleksandrov, V. V. Osiko, A. M. Prokhorov, and V. M. Tatarintsev, *ibid.* No. 12, 40 (1973).

[78] A. G. Merzhanov, V. A. Raduchev, and E. N. Rumanov, Dokl. Akad. Nauk SSSR **253**, 330 (1980) [Sov. Phys. Dokl. **25**, 565 (1980)].

[79] Yu. D. Kalafati, I. A. Serbinov, and L. A. Ryabova, Pis'ma Zh. Eksp. Teor. Fiz. **29**, 607 (1979) [JETP Lett. **29**, 583 (1979)].

[80] Stabilization of Superconducting Magnetic Systems (in Russian), Energiya, M., 1975.

[81] L. V. Keldysh, Vestn. MGU Ser. Fiz. Astron. **19** (4), 86 (1978).

[82] V. F. Elesin and Yu. V. Kopaev, Usp. Fiz. Nauk **133**, 259 (1981) [Sov. Phys. Usp. **24**, 116 (1981)].

[83] A. F. Volkov and Sh. M. Kogan, Usp. Fiz. Nauk **96**, 633 (1968) [Sov. Phys. Usp. **11**, 881 (1968)].

[84] A. F. Volkov and Sh. M. Kogan, Pis'ma Zh. Eksp. Teor. Fiz. **19**, 9 (1974) [JETP Lett. **19**, 4 (1974)].

[85] V. V. Grachev and E. N. Rumanov, Zh. Prikl. Mekh. Tekh. Fiz. No. 1, 44 (1984) [J. Appl. Mech. Tech. Phys. (USSR) No. 1 (1984)].

[86] V. V. Grachev and E. N. Rumanov, Dokl. Akad. Nauk SSSR **263**, 618 (1982) [Sov. Phys. Dokl. **27**, 261 (1982)].

[87] L. V. Mashkinov, Yu. E. Volodin, V. V. Barelko, and L. N. Gal'perin, Prib. Tekh. Eksp. No. 3, 140 (1975) [Instrum. Exp. Tech. **18**, 965 (1975)].

[88] V. V. Barelko and Yu. E. Volodin, Dokl. Akad. Nauk SSSR **211**, 1373 (1973) [Dokl. Phys. Chem. **211**, 673 (1973)].

[89] V. V. Grachev and E. N. Rumanov, *ibid.* **258**, 1147 (1981) [Dokl. Phys. Chem. **258** (1981)].

[90] G. I. Barenblatt and Ya. B. Zel'dovich, Usp. Mat. Nauk **26**, No. 2, 115 (1971) [Russ. Math. Surv. **26**, 45 (1971)].

[91] G. I. Barenblatt, Ya. B. Zel'dovich, V. B. Librovich, and T. M. Makhviladze, The Mathematical Theory of Combustion and Explosion, Consultants Bureau, N. Y., 1985 [Russ. original, Nauka, M., 1981].

[92] V. G. Voronkov and N. N. Semenov, Zh. Fiz. Khim. **19**, 1895 (1939).

[93] B. I. Makshantsev and V. M. Finkel'berg, Dokl. Akad. Nauk SSSR **217**, 1281 (1974) [Sov. Phys. Dokl. **19**, 516 (1974)].

[94] H. P. Broida and I. R. Pellam, Phys. Rev. **95**, 845 (1954).

[95] V. A. Shklovskiĭ, Zh. Eksp. Teor. Fiz. **82**, 536 (1982) [Sov. Phys. JETP **55**, 311 (1982)].

[96] A. G. Merzhanov, V. V. Barelko, I. I. Kurochka, and K. G. Shkadinskiĭ, Dokl. Akad. Nauk SSSR **221**, 1114 (1975) [Dokl. Phys. Chem. **221**, 366 (1975)].

[97] S. A. Zhukov, V. V. Barelko, and A. G. Merzhanov, *ibid.* **240**, 94 (1979) [Sov. Phys. Dokl. **24**, 205 (1979)].

[98] A. V. Gurevich and R. G. Mints, Usp. Fiz. Nauk **142**, 61 (1984) [Sov. Phys. Usp. **27**, 19 (1984)].

[99] Ya. B. Zel'dovich, Zh. Eksp. Teor. Fiz. **11**, 159 (1941).

[100] B. V. Novozhilov and V. S. Posvyanskiĭ, Fiz. Gor. Vzryva **9**, No. 2, 225 (1973).

[101] A. V. Kudryashov and V. G. Yakhno, Dynamics of Biological Systems (in Russian), IPF AN SSSR, Gor'kiĭ, 1978, No. 2, p. 45.

[102] A. C. Scott, *Active and Nonlinear Wave Propagation in Electronics*, Wiley, N. Y., 1970 [Russ. transl., Sov. radio, M., 1977, p. 285].

[103] F. V. Bunkin, V. I. Konov, A. M. Prokhorov, and V. B. Fedorov, Pis'ma Zh. Eksp. Teor. Fiz. **9**, 609 (1969) [JETP Lett. **9**, 371 (1969)].

[104] Yu. P. Raĭzer, Zh. Eksp. Teor. Fiz. **61**, 222 (1971) [Sov. Phys. JETP **34**, 114 (1972)].

[105] A. P. Sukhorukov, R. I. Khokhlov, and É. N. Shumilov, Pis'ma Zh. Eksp. Teor. Fiz. **14**, 129 (1971) [JETP Lett. **14**, 161 (1971)].

[106] D. T. Alimov, I. V. Edvabnyĭ, and P. K. Khabibullaev, see Ref. 6, Vol. 1, Part. 1, p. 61.

[107] B. E. Khartsiev, *ibid.*, p. 23.

[108] Yu. P. Raĭzer, Usp. Fiz. Nauk **132**, 549 (1980) [Sov. Phys. Usp. **23**, 789 (1980)].

[109] E. N. Rumanov, Fiz. Gor. Vzryva **19**, No. 4, p. 92 (1983).

[110] B. F. Mul'chenko, Yu. P. Raĭzer, and V. A. Épshteĭn, Zh. Eksp. Teor. Fiz. **59**, 1975 (1970) [Sov. Phys. JETP **32**, 1069 (1971)].

[111] M. V. Gerasimenko, G. O. Kozlov, V. A. Kuznetsov, and V. A. Masyukov, Pis'ma Zh. Tekh. Fiz. **5**, 954 (1979) [Sov. Tech. Phys. Lett. **5**, 397 (1979)].

[112] B. A. Malomed and E. N. Rumanov, Dokl. Akad. Nauk SSSR **284**, 1355 (1985) [Sov. Phys. Dokl. **30**, 872 (1985)].

[113] Ya. B. Zel'dovich and D. A. Frank-Kamenetskiĭ, *ibid.* **19**, 633 (1938).

[114] Ya. B. Zel'dovich, Zh. Eksp. Teor. Fiz. **9**, 1530 (1939).

[115] A. G. Merzhanov and A. E. Averson, Comb. Flame **16**, 89 (1971).

[116] A. G. Merzhanov, B. I. Khaĭkin, and K. G. Shkadinskiĭ, Zh. Prikl. Mekh. Tekh. Fiz. No. 5, 42 (1969) [J. Appl. Mech. Tech. Phys. (USSR) No. 5 (1969)].

[117] V. I. Ermakov, A. G. Strunina, and V. V. Barzykin, Fiz. Gor. Vzryva **14**, No. 6, 36 (1978).

[118] Ya. B. Zel'dovich, G. I. Barenblatt, and A. G. Istratov, Zh. Prikl. Mekh. Tekh. Fiz. No. 4, 66 (1962) [J. Appl. Mech. Tech. Phys. (USSR) No. **4** (1962)].

[119] G. M. Makhviladze and B. V. Novozhilov, *ibid.* No. 5, 440 (1971) [J. Appl. Mech. Tech. Phys. (USSR) No. 5 (1971)].

[120] E. I. Maksimov and K. G. Shkadinskiĭ, Fiz. Gor. Vzryva **7**, No. 3, 454 (1971).

[121] A. P. Aldushin and S. G. Kasparyan, Dokl. Akad. Nauk SSSR **244**, 67 (1979) [Sov. Phys. Dokl. **24**, 29 (1979)].

[122] G. I. Barenblatt and Ya. B. Zel'dovich, Prikl. Mat. Mekh. **21**, 856 (1957) [J. Appl. Math. Mech. (USSR) **21** (1957)].

[123] B. E. Petersen and H. W. Emmons, Phys. Fluids **4**, 456 (1961).

[124] Ya. B. Zel'dovich, Zh. Prikl. Mekh. Tekh. Fiz. No. 1, 102 (1966) [J. Appl. Mech. Tech. Phys. (USSR) No. 1 (1966)].

[125] A. P. Aldushin, S. G. Kasparyan, and K. G. Shkadinskiĭ, Dokl. Akad. Nauk SSSR **247**, 1112 (1979) [Sov. Phys. Dokl. **24**, 636 (1979)].

[126] A. F. Belyaev and L. D. Komkova, Zh. Fiz. Khim. **80**, 1302 (1950).

[127] A. G. Merzhanov, Vestn. Akad. Nauk SSSR No. 10, 30 (1981).

[128] A. P. Aldushin, T. M. Martem'yanova, A. G. Merzhanov, B. I. Khaĭkin, and K. G. Shkadinskiĭ, Fiz. Gor. Vzryva **9**, No. 5, 613 (1973).

[129] G. I. Barenblatt, Combustion and Explosion (in Russian), Nauka, M., 1972, p. 15.

[130] G. P. Andrianova, V. A. Kargin, and A. S. Kachek'yan, Vysokomol. Soedin. **12**, 8 (1970).

[131] Yu. M. Maksimov, A. T. Pak, G. V. Lavrenchuk, D. S. Naĭborodenko, and A. G. Merzhanov, Fiz. Gor. Vzryva **15**, No. 3, 156 (1979).

[132] Yu. M. Maksimov, A. G. Merzhanov, A. T. Pak, and M. N. Kuchin, *ibid.* **17**, No. 4, 51 (1981).

[133] V. A. Vol'pert, A. I. Vol'pert, and A. G. Merzhanov, Dokl. Akad. Nauk SSSR **263**, 918 (1982) [Dokl. Phys. Chem. **263** (1982)].

[134] V. A. Vol'pert, "Bifurcation of nonstationary wave propagation states" (in Russian), Preprint OIKhF AN SSSR, Chernogolovka, 1982.

[135] V. A. Vol'pert, A. V. Dvoryankin, and A. G. Strunina, Fiz. Gor. Vzryva **19**, No. 4, 10 (1983).

[136] A. G. Merzhanov, A. V. Dvoryankin, and A. G. Strunina, Dokl. Akad. Nauk SSSR **267**, 869 (1982) [Dokl. Phys. Chem. **267** (1982)].

[137] A. G. Strunina, A. V. Dvoryankin, and A. G. Merzhanov, Fiz. Gor. Vzryva **19**, No. 2, 30 (1983).

[138] E. Schrödinger, *What is Life? The Physical Aspect of the Living Cell*, Cambridge University Press, 1967 [Russ. transl. of earlier ed., IL, M., 1947].

[139] R. M. Zaĭdel' and Ya. B. Zel'dovich, Zh. Prikl. Mekh. Tekh. Fiz. No. 4, 28 (1962) [J. Appl. Mech. Tech. Phys. (USSR) No. 4 (1962)].

[140] A. G. Merzhanov and A. K. Filonenko, Dokl. Akad. Nauk SSSR **152**, 143 (1963) [Dokl. Phys. Chem. **152**, 769 (1963)].

[141] A. G. Merzhanov, V. A. Raduchev, and E. N. Rumanov, Zh. Prikl. Mekh. Tekh. Fiz. No. 1, 7 (1985) [J. Appl. Mech. Tech. Phys. (USSR) No. 1 (1985)].

[142] M. B. Borovnikov, M. A. Burovoĭ, U. I. Gol'dshleger, and A. G. Merzhanov, Dokl. Akad. Nauk SSSR **272**, 327 (1983) [Sov. Phys. Dokl. **28**, 758 (1983)].

[143] E. A. Nekrasov and A. M. Timokhina, Fiz. Gor. Vzryva **20**, No. 4, 21 (1984).

[144] A. A. Zenin and G. A. Nerisyan, "Thermal structure of an SVS wave in Ti-Si and Zr-Si systems" (in Russian), Preprint OIKhF AN SSSR, Chernogolovka, 1980.

[145] A. P. Aldushin, A. G. Merzhanov, and B. I. Khaĭkin, Dokl. Akad. Nauk SSSR **204**, 1139 (1972) [Dokl. Phys. Chem. **204**, 475 (1972)].

[146] A. F. Belyaev, Zh. Fiz. Khim. **14**, 1009 (1940).

[147] P. F. Pokhil, Zh. Fiz. Gor. Vzryva No. 2, 181 (1953).

[148] B. I. Khaĭkin and A. G. Merzhanov, Dokl. Akad. Nauk SSSR **173**, 1382 (1967) [Dokl. Phys. Chem. **173**, 295 (1967)].

[149] O.B. Yakusheva, E. I. Maksimov, and A. G. Merzhanov, Fiz. Gor. Vzryva **3**, No. 3, 125 (1966).

[150] E. N. Rumanov and B. I. Khaikin, *ibid.* **18**, No. 6, 24 (1982).

[151] S. I. Anisimov, M. I. Tribel'skii, and Ya. G. Épel'baum, Zh. Eksp. Teor. Fiz. **78**, 159 (1980) [Sov. Phys. JETP **51**, 802 (1980)].

[152] A. G. Merzhanov, I. P. Borovinskaya, and Yu. E. Volodin, Dokl. Akad. Nauk SSSR **206**, 905 (1972) [Dokl. Phys. Chem. **206**, 905 (1972)].

[153] A. P. Aldushin, A. G. Merzhanov, and B. I. Khaikin, *ibid.* **215**, 612 (1974) [Dokl. Phys. Chem. **215**, 295 (1974)].

[154] E. N. Rumanov, Pis'ma Zh. Eksp. Teor. Fiz. **35**, 286 (1982) [JETP Lett. **35**, 354 (1982)].

[155] F. V. Bunkin, N. A. Kirichenko, and B. S. Luk'yanchuk, Usp. Fiz. Nauk **138**, 45 (1982) [Sov. Phys. Usp. **25**, 662 (1982)].

[156] A. M. Bonch-Bruevich and M. N. Libenson, Abstracts of Papers Presented at the Second All-Union Symposium on Laser Chemistry (in Russian), Zvenigorod, 1980, p. 71.

[157] Yu. M. Romanovskiĭ, N. B. Stepanova, and D. S. Chernavskiĭ, Mathematical Biophysics (in Russian), Nauka, M., 1984, Chap. 3.

[158] J. Taffanael, C. R. Bull. Chim. Soc. **157**, 714 (1913); **158**, 42.

[159] Ya. B. Zel'dovich, Dokl. Akad. Nauk SSSR **257**, 1173 (1981) [Dokl. Phys. Chem. **257** (1981)].

[160] Ya. B. Zel'dovich and Yu. A. Zysin, Zh. Tekh. Fiz. **11**, 501 (1941).

[161] V. G. Abramov and A. G. Merzhanov, Teor. Osnovy Khim. Tekhnol. **9**, 863 (1975).

[162] V. V. Barelko, V. M. Beĭbutyan, Yu. E. Volodin, and Ya. B. Zel'dovich, Dokl. Akad. Nauk SSSR **257**, 339 (1981) [Sov. Phys. Dokl. **26**, 335 (1981)].

[163] A. P. Aldushin, V. D. Lugovoĭ, A. G. Merzhanov, and B. I. Khaĭkin, *ibid.* **243**, 1434 (1978) [Sov. Phys. Dokl. **23**, 914 (1978)].

[164] A. P. Aldushin, Ya. B. Zel'dovich, and S. I. Khudyaev, Fiz. Gor. Vzryva **15**, No. 6, 20 (1979).

[165] L. S. Polak and A. S. Mikhaĭlov, Self-Organization in Nonequilibrium Physicochemical Systems (in Russian), Nauka, M., 1983.

[166] N. M. Kuznetsov, Zh. Eksp. Teor. Fiz. **49**, 1526 (1965) [Sov. Phys. JETP **22**, 1047 (1966)].

[167] Ya. B. Zel'dovich, A. G. Istratov, N. I. Kidin, and V. B. Librovich, Combust. Sci. Technol. **24**, 1 (1980).

[168] K. I. Shchelkin and L. G. Troshin, Gas Dynamics of Combustion (in Russian), Nauka, M., 1963.

[169] R. I. Soloukhin, Usp. Fiz. Nauk **80**, 525 (1963) [Sov. Phys. Usp. **6**, 523 (1963)].

[170] Ya. B. Zel'dovich and V. V. Rachinskiĭ, Introduction to the General Theory of the Dynamics of Sorption and Chromatography (in Russian), Nauka, M., 1964.

[171] Ya. B. Zel'dovich, Elektrokhimiya **13**, 677 (1977).

[172] Ya. B. Zel'dovich and A. A. Ovchinnikov, Pis'ma Zh. Eksp. Teor. Fiz. **26**, 588 (1977) [JETP Lett. **26**, 440 (1977)].

[173] Ya. B. Zel'dovich and A. A. Ovchinnikov, Zh. Eksp. Teor. Fiz. **74**, 1588 (1978) [Sov. Phys. JETP **47**, 829 (1978)].

Translated by S. Chomet